FATIGUE TESTS OF HYBRID PLATE GIRDERS
UNDER COMBINED BENDING AND SHEAR

by

David J. Fielding
A. A. Toprac

Research Report Number 96-2

Fatigue Strength of Hybrid
Plate Girders Under Shear

Research Project Number 3-5-66-96

conducted for

The Texas Highway Department

by the

CENTER FOR HIGHWAY RESEARCH

THE UNIVERSITY OF TEXAS

AUSTIN, TEXAS

July 1967

## ACKNOWLEDGMENTS

This is the second of three reports that describe the work in Research Study No. 3-5-66-96, entitled "Fatigue Strength of Hybrid Plate Girders Under Shear." The first report issued is Report No. 96-1, entitled "Additional Fatigue Tests of Hybrid Plate Girders Under Pure Bending Moment." The Third report will be prepared and issued after the completion of tests presently under way.

ABSTRACT

Three hybrid plate girders were tested in combined bending and shear. Both fatigue and static ultimate tests were performed. The flanges were of A514 steel and the webs were of A36 steel. The stress range in the flanges was 25 ksi with the flange stress fluctuating from 25 ksi to 50 ksi. The only variable was the transverse stiffener length. From the tests it is concluded that the U-shaped cracks that formed under the stiffeners in one girder were not fatal and that hybrid plate girders under combined bending and shear have a shorter fatigue life than the same girders under pure bending. From the static ultimate tests it is concluded that Basler's tension field theory can be used to predict the ultimate load of hybrid plate girders under combined bending and shear.

# TABLE OF CONTENTS

# 1. INTRODUCTION

Because the hybrid plate girder can be of economic value, research is being conducted at The University of Texas to determine how these structures behave and to formulate design rules for them. The test program was begun in 1960 with preliminary static-behavior tests and continued with preliminary fatigue tests in 1963. The results of these tests have been published. [1, 2, 3, 4] The tests being presented here are a part of the overall test program to determine the fatigue and static behavior of hybrid plate girders.

Fatigue tests and static ultimate tests were run on three hybrid plate girders with ASTM A514 steel flanges and A36 steel webs. The loading configuration was such that the interaction of bending and shear can be studied. The purpose of this report is to present the test program and the experimental results of these tests and to determine how the results compare with those of previous tests. [1, 2, 3, 4] The effect of transverse-stiffener length is also investigated.

## 2. TEST PROGRAM

### 2.1 Introduction

The primary purpose of these tests was to examine the effect of shear stress combined with bending stress on the fatigue behavior of hybrid plate girders and to explore how different lengths of transverse stiffeners influence fatigue strength. Few differences among the results of these tests were expected because the girders were identical in all details except transverse-stiffener length. Two of these girders had stiffeners cut 2 in. short of the tension flange and the third had an 8-inch cutoff.

### 2.2 Test Specimens

Figure 1 shows girder geometry, nominal plate sizes, stiffener locations, and weld sizes. The two girders, 32550-C2 and 32550-C2R were identical, and girder 32550-C1 was different from these two only in the length of the transverse stiffeners. Only the end-bearing stiffeners were full-length. The two stiffeners in the middle three panels intentionally had an 8-inch cutoff in all girders to prevent fatigue cracks in the web at the toe of stiffener-to-web weld near the tension flange.

The girder designations are

32550-C2,

32550-C2R, and

32550-C1.

The first digit gives the web thickness in sixteenths of an inch. The next four numbers give the minimum and maximum extreme fiber stresses of the fatigue test. The "C" is used to designate the test series. In the "C" series, aspect ratios (ratio of panel width to depth) were 1.0 for all girders. The next digit, either a 1 or a 2, indicates the stiffener cutoff length of 8 in. or 2 in., respectively. An R following the stiffener designation identifies a duplicate girder. The only variable parameter in these tests was the stiffener length.

The flanges were of ASTM A514 steel and the webs were of A36 steel. The flanges were 8 in. by 1/2 in. plates; the webs were 36 in. deep and 3/16 in. thick. The cross section is shown in Fig. 2 with an 8-inch cutoff shown by dashed lines. The panels designated S1 through S6 in Fig. 3 were the test panels and these had aspect ratios of 1.0. The three central panels had smaller aspect ratios to limit web deflections. Six-inch end-post panels were used for all girders.

Actual plate dimensions as measured in the laboratory are given in Table 1. The flange width and thickness were obtained from measurements made at 31 locations on the flanges of each girder. The web thickness was obtained from measurements made on a coupon plate cut from the same plate that was used for the web. The nominal plate dimensions give a web-slenderness ratio, (ratio of web depth to thickness), of 192. The actual ratios are shown in Table 1. It should be noted here that the mill scale on the flanges was quite thick (about 0.005 inch) and that no attempt was made to remove it or adjust the measurements where thickness measurements were made.

To determine the static yield point (at zero strain rate) of the steel, standard tensile tests were made on specimens from the coupon plates. Two tensile specimens were cut from each coupon plate; one perpendicular and one parallel to the direction of rolling of the web plate. Tensile specimens were cut parallel to the direction of rolling of the flange plate. The static yield point, percent elongation in 8 in., and chemical composition from the mill report are given in Table 2.

## 2.3 Test Setup and Instrumentation

The girders were simply supported at their ends and subjected to equal loads applied through hydraulic jacks as shown schematically in Fig. 3. A pulsator and hydraulic jacks of 120 kips dynamic capacity and 160 kips static capacity were used to apply cyclic loads in the fatigue tests and static loads in the ultimate-load tests. Sufficient lateral bracing was provided to prevent lateral buckling of the compression flange. The locations of lateral bracing are indicated in Fig. 3.

Deflections were measured at the supports, load points, and centerline. Lateral web deflections were measured with a moveable head dial rig. Panel S3 (See Fig. 3) was instrumented with electrical-resistance rosette strain gages for the static-ultimate test of 32550-C2R. Gage locations are described in Chapter 3 where the strains are discussed. In addition, the girders were whitewashed so that yielding could be observed During the fatigue tests the slip deflection was measured at the

centerline of the girder. Slip deflection is the increase in the deflection measured at the maximum fatigue-test load.

## 2.4 Reference Loads

When the extreme-fiber flange stress is 50 ksi an A36 steel web should be partially yielded. This means that the linear stress distribution must be modified to calculate the loads that are required to give extreme flange-fiber stresses of any magnitude since the stress distribution is permanently affected after the first load cycle (See Section 3.1).

$P_{min}$ and $P_{max}$ are given in Table 3 from the stress distributions of Fig. 4d and c, respectively. The load that produces first yielding in the web, $P_{yw}$, the theoretical ultimate load, $P_u^{th}$, and the load to produce plastic moment, $P_p$, are also tabulated. Theoretical ultimate loads were calculated according to References 5, 6, and 7, considering the interaction of bending and shear stresses. Figure 5 shows the interaction diagram between moment and shear and the ray drawn from the origin of axes represents the loading condition of the test girders. The heavier portion of this ray indicates the fatigue-test range.

## 3. TEST PROCEDURE AND RESULTS

### 3.1  Loading History and Procedure

Figures 6 and 7 are load-versus-centerline-deflection curves for Girder 32550-C2.  These provide a convenient reference for discussion of the procedure.  Figure 6 is the load-versus-centerline-deflection curve for the preliminary load cycle prior to the fatigue test.  The specimen was loaded first under static load to $P_{max}$ (Load No. 8) in predetermined intervals at which time strain readings, girder deflections, and lateral web deflections were measured.  Load numbers were assigned whenever loading was stopped to record strains and deflections.  Then the girder was unloaded to $P_{min}$ (Load No. 11) and the same data was taken.

The purpose of this preliminary cycle was to obtain the deflected web patterns at $P_{min}$ and $P_{max}$.  Data at $P_{min}$ was taken after $P_{max}$ was attained because the stress distribution changes when the web yields.  This is shown in Fig. 4 where successive stress distributions are shown from the original zero load (Load No. 1) in Fig. 4a to the final zero load (load No. 14) in Fig. 4e.  If welding residual stresses are not considered, the stresses originally in the cross section are as in Fig. 4a which corresponds to Load No. 1 in Fig. 6.  The stress distribution is linear (Fig. 4b) until the web begins to yield.  Loading continues to $P_{max}$ (Load No. 8) where the stress distribution is as shown in Fig. 4c.  Load No. 11, $P_{min}$, gives the stress distribution of Fig. 4d which is not the same as

that of Load No. 4, $P_{min}$. When the load is reduced further to zero, the stress distribution is as shown in Fig. 4e rather than 4a because of the inelastic distortions that have occurred due to yielding in the web.

After the preliminary loading cycle, fatigue testing was begun. The three specimens were tested at the rate of 260 cycles per minute. Inspections were made every three hours (or more frequently) to determine the time and location of the first and all succeeding cracks and to measure crack propagation. The cracks were numbered consecutively in the order of discovery.

If a crack formed on the tension side (below the neutral axis) of the girder it was permitted to propagate until it entered the tension flange. When a crack entered the tension flange it was repaired by the "arc-air" method and testing was resumed. However, once a crack was repaired it usually re-opened after testing was resumed, thus pointing out the fatal nature of a crack in the tension area of a plate girder.

After the fatigue test was halted, all cracks were repaired in order that the girder could be tested to its static ultimate load. Figure 7 is the load-versus-centerline-deflection curve for the static ultimate test on Girder 32550-C2. At Load No. 15 in Fig. 7, zero readings were taken on strain gages and deflection gages. Then the load was increased in predetermined intervals until inelastic behavior was noted; then smaller increments were applied.

After failure, the load was returned to zero. Figure 8 is the load-versus-centerline-deflection curve for the ultimate load test on 32550-C2R.

## 3.2 Fatigue Test Results

### Introduction

Web Deflections, measured at $P_{max}$ and $P_{min}$, for panel S3 or S4 of each specimen are shown in Figs. 9 through 11. These are presented here only to show the magnitude of the deflection of the web plates in critical test panels (high moment and shear).

### Girder 32550-C2

In the preliminary static test (Fig. 6) yielding was first observed in the web directly under the loading jacks at 64 kips. At Load No. 7 (80 kips) random localized yielding of the web was noted in panels B1 and B3. Since the actual yield point of the web steel was 51.22 ksi none of the web should have yielded; however, the presence of welding-residual stresses made yielding of some portions entirely possible at low loads.

A fatigue test was run with the load fluctuating between 45.3 kips and 90.6 kips to produce minimum and maximum extreme fiber stresses of 25 and 50 ksi, respectively. The first crack was noted at 316,000 cycles in the web at the web-to-compression flange fillet weld. At 387,000 cycles, a second crack formed at the transverse stiffener-to-web fillet weld. These locations are shown

in Fig. 12. At 567,000 cycles Crack No. 2 entered the tension flange.

Crack No. 2 was repaired and testing was resumed until 601,000 cycles at which time Crack No. 2 reopened and a third crack was noticed. Crack No. 3 was similar to Crack No. 1. The propagation curves of Cracks No. 1 and 2 are plotted in Figs. 13 and 14.

## Girder 32550-C2R

The preliminary static test showed that this girder behaved the same as did 32550-C2 (Fig. 8). In the fatigue test three cracks (Cracks 1, 2, 5) were found in the web at the toe of the transverse stiffener-to-web fillet weld as shown in Fig. 15. Cracks 3 and 4 occurred at flange-web weld discontinuities. The first crack was noted at 603,000 cycles. After repeated repairing of the cracks at the bases of the stiffeners, Crack No. 6 was observed at the toe of the compression flange-to-web weld. Cracks 3 and 4 in Fig. 15 were the result of defective welding because they formed in the weld rather than in the web plate.

## Girder 32550-C1

The behavior in the preliminary static test was like that of 32550-C2 except that the initial web deflections (Fig. 11) were much greater in the bottom (or tension) half of the girder. This girder had "short" stiffeners and the first fatigue crack was noted

at 60,000 cycles at the bottom of a stiffener as shown in Fig. 16. This was a U-shaped crack in the web at the base of the weld. Cracks No. 3 and 4 were also of this type. The latter crack is shown in Fig. 17. Once formed, this type of crack propagated so slowly that the growth of crack is believed to have stopped. The vertical stiffeners of 32550-C1 could be seen moving laterally at their cutoff ends as a result of lateral web movement. The cracks at the bottoms of stiffeners appeared first on the tension face of the breathing web plate. The tension face can be determined from Fig. 11.

Crack No. 2 was a transverse stiffener-to-web weld crack forming first at the cutoff end of the stiffener as in the case of the two previous girders. However, in this girder, failure was not caused by this crack gradually penetrating the tension flange. In fact, Crack No. 2 progressed upward as fast and as much as it progressed downward. The progress of this crack in panel S4 can be seen in Fig. 18. Also in this panel, at 412,000 cycles, Crack No. 5 was noticed in the web at the web-to-compression-flange weld. This crack grew as shown in Fig. 18 and became so long that the top of the web was buckled out of its plane and was completely separated from the flange. Nevertheless, testing was continued to see whether or not Crack No. 2 would eventually enter the tension flange. However, at 634,000 cycles another crack (Crack No. 8) formed in panel S4 near the neutral axis, and it too grew both upward and downward until it met Crack No. 2. When the two cracks met, the panel had virtually no stiffness and the centerline slip-deflection increased rapidly. Figure 19 shows the failed panel. The horizonal

arrow shows where the two cracks met and the vertical arrows mark the extremities of Crack No. 5. Figure 20 shows the gradual loss of stiffness in a cycles-versus-slip diagram. The first two girders with only 2-inch cutoff did not exhibit this gradual loss of stiffness (i. e. , the slip-deflection was zero). The crack propagation curves for Cracks No. 2 and 5 are given in Figs. 21 and 22.

At the same time that Cracks No. 2, 5, and 8 were propagating in panel S4, similar behavior was noted in panel S3 (Fig. 16), Crack No. 3 was one of the U-shaped cracks that did not grow visibly and in no way resembled Crack No. 2.

### 3.3 Static Load-Tests

### Girder 32550-C2

Yielding along the tension diagonals was visible at Load No. 25 (Fig. 7) in panels S3 and S4. By the time Load No. 28 was reached tension-diagonal yielding was visible in all six test panels. It is questionable whether these were diagonals extending from one corner to the opposite one or whether principal yielding was along a line at an an angle less than that of the diagonal. The ultimate load was 153.6 kips. Figure 23 shows the girder after failure. The total deformation is small because after ultimate load was attained the load dropped off rapidly. Figure 24 shows the shear failure in panel S3.

The web deflections for this girder are shown in Fig. 9 at zero load, $P_{min}$, and $P_{max}$ of the fatigue test, and at 144 kips.

These show the typical web deflection behavior for girders subjected to high moment and shear. A buckling valley forms extending from the upper left corner of the panel to just about the lower right corner; whereas, in high shear the valley extends from corner to corner.[6]

## Girder 32550-C2R

Panel S4 was stiffened with a diagonal stiffener after the fatigue test in an attempt to force a failure in panel S3 which was instrumented with rosette strain gages. At Load No. 24 (Fig. 8) tension-field yielding along a line at an angle less than that of the diagonal was noted in all panels (Fig. 25). A shear failure occurred at 148.0 kips in panel S5 as shown in Fig. 26. The portion of the load-deflection curve (Fig. 8) beyond Load No. 25 was not obtained but $P_u^{ex}$ was the maximum load that was applied to the specimen.

The principal stresses at the center of panel S3 are shown in Fig. 27. Beam-theory stresses and the theoretical web buckling stress are indicated. Also shown in Fig. 27 is the orientation of the principal stresses as the load increased; beam theory predicts a constant inclination of $45^\circ$.

Strains in the regions of tension-field anchorage were also measured. These were converted to stresses and plotted in Fig. 28. The rosette-gage location is shown in a sketch on the figure and its coordinates marked. The origin is at the geometric center of the panel. The inclination of the principal tensile stress is also given in Fig. 28.

## Girder 32550-C1

Panel S4 was damaged extensively in the fatigue test and a repair was not possible, so there was no static-ultimate load test of this specimen.

## 4. DISCUSSION

### 4.1 Fatigue Cracks

Three distinct types of cracks were defined in Reference 3. These are summarized in the Nomenclature section of this study, together with two additional types of cracks.

Type 1 cracks formed at the toe of the compression flange-to-web weld. These cracks form where the secondary bending stresses due to lateral web deflection are greatest. Actual magnitudes of secondary bending strains in the region of these cracks are difficult to ascertain but can be approximately calculated from web-deflection data as explained in Reference 8.

Type 2 cracks began at the toe of the transverse stiffener-to-web weld at the cutoff end of the stiffener. These cracks lead eventually to fracture of the tension flange where the cutoff was 2 in. Figures 14 and 21 show the propagation of Type 2 cracks. These cracks progressed faster with time. Figures 13 and 22 show the propagation of Type 1 cracks which grow gradually to reduce the stiffness of the girder web and caused failure in 32550-C1 only by growing so large that the web became ineffective.

Cracks No. 3 and 4 in 32550-C2R were Type 3 cracks. These occurred at weld discontinuities.

A new type of crack (Type 4) began around the bottom of the short stiffeners (Girder 32550-C1 only). Type 4 cracks were noted very early in the fatigue test of 32550-C1; however, these cracks grew very slowly and were not the cause of fracture of the girder.

These cracks are not dangerous because in 32550-C1 the first crack at 60,000 cycles was a Type 4 crack, but the final fracture of the girder was at 745,000 cycles. The failure was not caused by the Type 4 crack.

Another type of crack (Type 5) was found in the specimen with short stiffeners. Type 5 cracks began at the middepth of the girder at the toe of the transverse stiffener-to-web weld. These cracks (Cracks No. 7 and 8 in Fig. 16) are evidently caused by web flexing. They formed when the web panels had already lost much of their stiffness due to Types 1 and 2 cracks. However, in 32550-C1 the combination of a Type 5 crack and a Type 2 crack caused failure.

In Reference 3 an S-N curve for hybrid plate girders in pure bending was presented. This curve is reproduced here as Fig. 29. The results of the tests in combined bending and shear are also plotted in Fig. 29. It is evident that the combined bending and shear-stress state results in shorter fatigue life than predicted by the curve of Reference 3. The life of Specimen 32550-C1 is taken as 204,000 cycles because the first crack (Type 4) is considered to be solely the result of terminating the stiffeners 8 inches above the tension flange. Furthermore, Type 4 cracks do not seem to be of any significance as far as fatigue life is concerned. However, the Type 2 crack that formed at 204,000 cycles may have formed early due to the lack of web stiffening ability of the stiffeners with an 8-inch cutoff. Insufficient data is available to draw any conclusions on this point.

## 4.2 Stiffener Length

The reason for cutting off the stiffeners 2 in. above the tension flange was to avoid the necessity of welding on or near the flange since welding is known to cause residual tensile stresses detrimental to fatigue life. The 8-inch cutoff in Specimen 32550-C1 was tried to move the welding-residual stress at the end of the stiffener even closer to the neutral axis, thus trying to prevent Type 2 cracks. Girders 32550-C2 and 32550-C2R were identical and experienced only Type 1 and Type 2 cracks in the test panels. Failure resulted when Type 2 cracks penetrated into the tension flange.

The 8-inch cutoff resulted in large lateral web deflections in the lower or tension area of the web. These are shown in Fig. 11 as compared with Figs. 9 and 11 for the other two girders. The first crack appeared in 32550-C1 at 60,000 cycles, a Type 4 crack evidently due to this excessive lateral web movement in the tension portion of the web. The number and locations of cracks in this specimen (Fig. 16) indicate a lack of stiffness of the web plate. Perhaps a stiffener cutoff between the 2-inch and the 8-inch cutoffs tested may result in a sufficiently stiffened web and a delayed formation of Type 2 cracks.

In Fig. 16, Crack No. 2 is a Type 2 crack in the specimen with short stiffeners, and it formed earlier than the Type 2 cracks in the two girders with longer stiffeners. However, at present there is insufficient data to draw any substantial conclusion from this observation.

## 4.3 Ultimate Loads

The reference loads and the experimental ultimate loads are given in Table 3. $P_{min}$ and $P_{max}$ refer to the fatigue tests. $P_{yw}$ is the load at which yielding of the web first occurs due to longitudinal primary bending strains. $P_p$ is the load which corresponds to the plastic moment. $P_u^{th}$ is the theoretical ultimate load given by Reference 7, considering the interaction between moment and shear. The treatment in Reference 7 is for homogeneous plate girders rather than for hybrid girders; however, the experimental ultimate loads agree well with the predictions for the homogeneous girders. The last line in Table 3 shows the ratios of $P_u^{ex}$, the experimental ultimate load, to $P_u^{th}$. The indication is that Basler's tension-field theory [5, 6, 7] works well for hybrid plate girders. This is not surprising considering that Basler's theory is a combination of three basic phenomena: compression-flange stability, web buckling, and tension-field development in the web; all of which can be treated separately as was done in References 5, 6, and 7. Figure 5 shows the loading-condition line (ray from origin with arrowhead) for the ultimate load tests (and the fatigue tests) on the interaction diagram. The slope of the loading-condition line is computed in the lower part of Fig. 5. The circled point where the loading-condition line intersects the interaction diagram gives the predicted ultimate load.

Tension-field theory basically says that the compressive diagonal stress increases until the critical buckling stress is

reached at which time the web buckles and thereafter the compressive diagonal stress remains essentially constant. At the same time, the tension diagonal stress can increase; it is not limited by buckling. Figure 27 shows this behavior for panel S3 of Specimen 32550-C2R. These stresses were determined from an elastic analysis of data from rosette gages at the geometric center of panel S3. The indication here is that tension-field theory can predict the behavior and ultimate load of hybrid girders. Figure 27 also shows the slope of the principal tensile stress which is inclined at $45^\circ$ or slightly steeper throughout the test. This indicates that the tension field lies along the diagonal of the panel. In Fig. 28 the angle $\phi$ started out at the beam-theory prediction, but as the load was increased the angle approached $45^\circ$. This also indicates that a tension "diagonal" forms in spite of the fact that the whitewash cracked along a line that was not the diagonal (Fig. 25).

# 5. CONCLUSIONS

1. Fatigue cracks forming at the toe of the transverse stiffener-to web weld propagated into the tension flange in the specimens with a 2-inch cutoff.

2. Failure of the specimen with an 8-inch stiffener cutoff was through loss of web stiffness rather than by tension-flange fracture.

3. The U-shaped cracks found in one test formed early in the girder life but were not fatal and remained stable through several hundred thousand cycles.

4. Hybrid plate girders under combined bending and shear appear to have a shorter fatigue life than the same girders under pure bending.

## 6. FATIGUE CRACK NOMENCLATURE

| Classification | Description |
| --- | --- |
| Type 1 - | Cracks forming at the toe of the compression flange-to-web weld. |
| Type 2 - | Cracks forming at the toe of the transverse stiffener-to-web weld at the cutoff end of the stiffener. |
| Type 3 - | Cracks beginning in the web-to-tension-flange weld resulting from any discontinuity or notch. |
| Type 4 - | U-shaped cracks around the bottom of "short" vertical stiffeners (Fig. 17). |
| Type 5 - | Cracks forming at the toe of the transverse stiffener-to-web weld at girder middepth. |

# 7. TABLES AND FIGURES

| GIRDER | 32550-C2 | 32550-C2R | 32550-C1 |
|---|---|---|---|
| Web Plate | 36" x 0.204" | 36" x 0.204" | 36" x 0.204" |
| Flange Plates | 7.981" x 0.532" | 7.985" x 0.532" | 7.998" x 0.534" |
| $\alpha$ | 1.0 | 1.0 | 1.0 |
| $\beta$ | 176.5 | 176.5 | 176.5 |

Table 1    Dimensions of Plates

| | Flange Steel | Web Steel |
|---|---|---|
| Yield Stress (ksi) | 106.24 | 51.22 |
| % Elongation (in 8 in.) | 14 | 24 |
| Chemical Composition (%) | | |
| C | 0.20 | 0.21 |
| Mn | 0.56 | 0.50 |
| P | 0.010 | 0.012 |
| S | 0.019 | 0.024 |
| Si | 0.30 | 0.10 |
| Cr | 1.01 | ---- |
| Mo | 0.21 | ---- |
| Cu | 0.33 | ---- |
| B | 0.002 | ---- |
| Ti | 0.068 | ---- |

Table 2    Properties of Plates

| Load (kips) | 32550-C2 | 32550-C2R | 32550-C1 |
|---|---|---|---|
| $P_{min}$ | 45.3 | 45.3 | 45.5 |
| $P_{max}$ | 90.6 | 90.6 | 91.0 |
| $P_{yw}$ | 95.6 | 95.6 | 96.0 |
| $P_p$ | 183.8 | 183.8 | 184.8 |
| $P_u^{th}$ | 153.4 | 153.4 | 153.4 |
| $P_u^{ex}$ | 153.6 | 148.0 | ----- |
| $P_u^{ex}/P_u^{th}$ | 1.00 | 0.96 | ----- |

Table 3

Reference-Loads and Tests-Loads

## SPECIMENS 32550-C2 & 32550-C2R

PL. 8"x1/2"(typ)(A514)

1/2"

3½"x1/2"
(typ)(A514)

3"x 3/16"
(typ)(A36)

36"x3/16"
WEB

3½"x 1/2"
(typ)(A514)

1/4

36"

3/16

3/16

1/4

8"

2"

PL. 8"x1/2"(typ)(A514)

1/2"

6" | 3'-0" | 3'-0" | 3'-0" | 1'-6" | 1'-8" | 1'-6" | 3'-0" | 3'-0" | 3'-0" | 6"

23'-8"

## SPECIMEN 32550-C1

36"x3/16"
WEB

8"

6" | 3'-0" | 3'-0" | 3'-0" | 1'-6" | 1'-8" | 1'-6" | 3'-0" | 3'-0" | 3'-0" | 6"

23'-8"

24
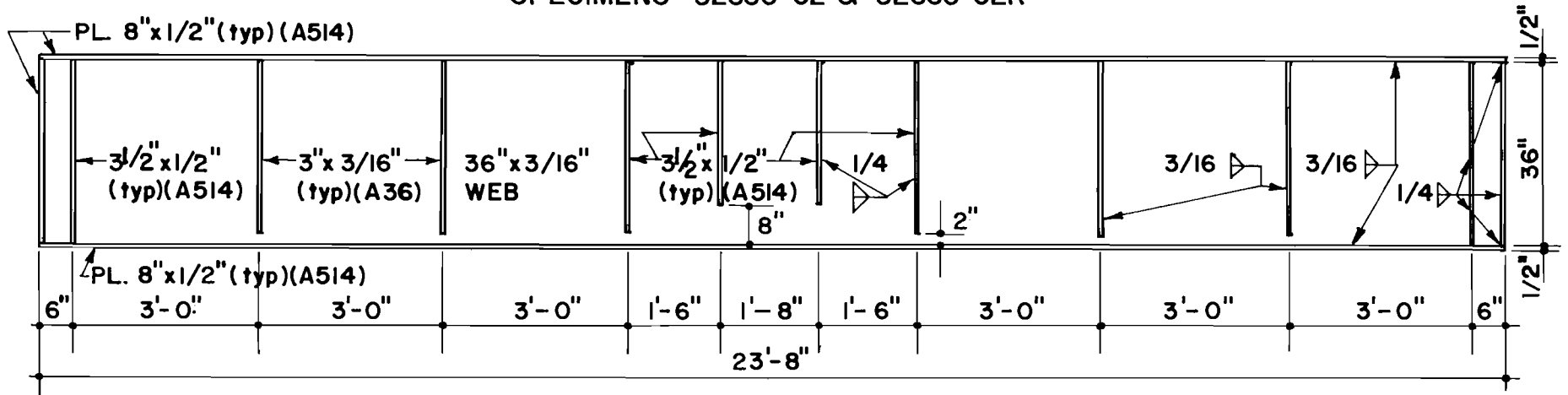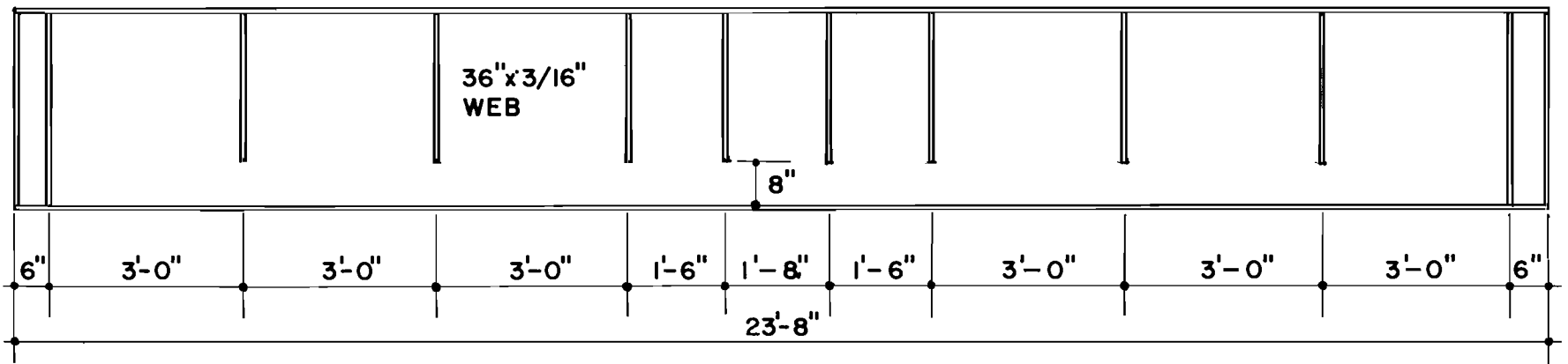
## FIG. I   TEST SPECIMENS
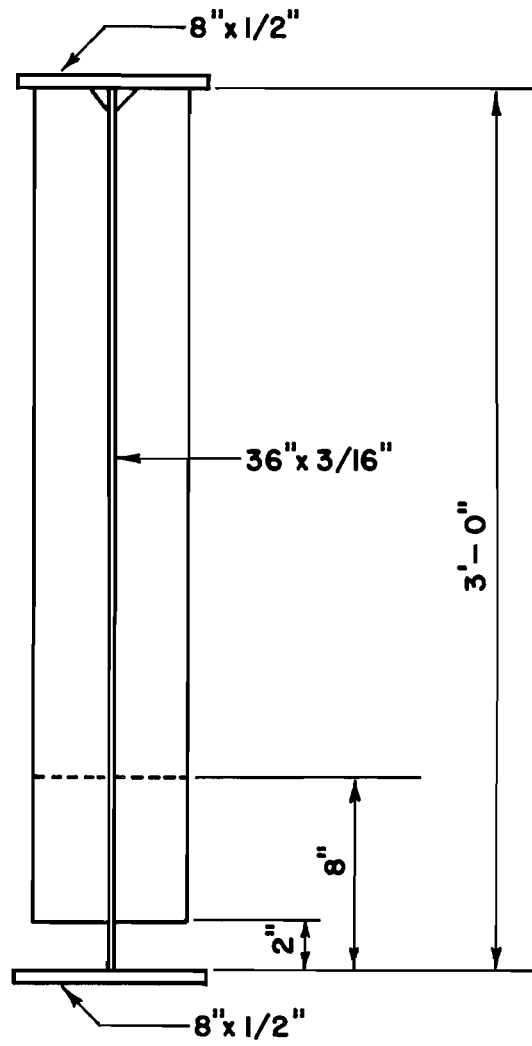
FIG. 2   TYPICAL  CROSS-SECTION

P       P

LATERAL SUPPORT POINTS

| S1 | S2 | S3 | B1 | B2 | B3 | S4 | S5 | S6 |

9'– 0"         4'– 8"         9'– 0"

22'– 8"

9P

MOMENT

+ P

– P

SHEAR

FIG. 3 TEST SETUP

26
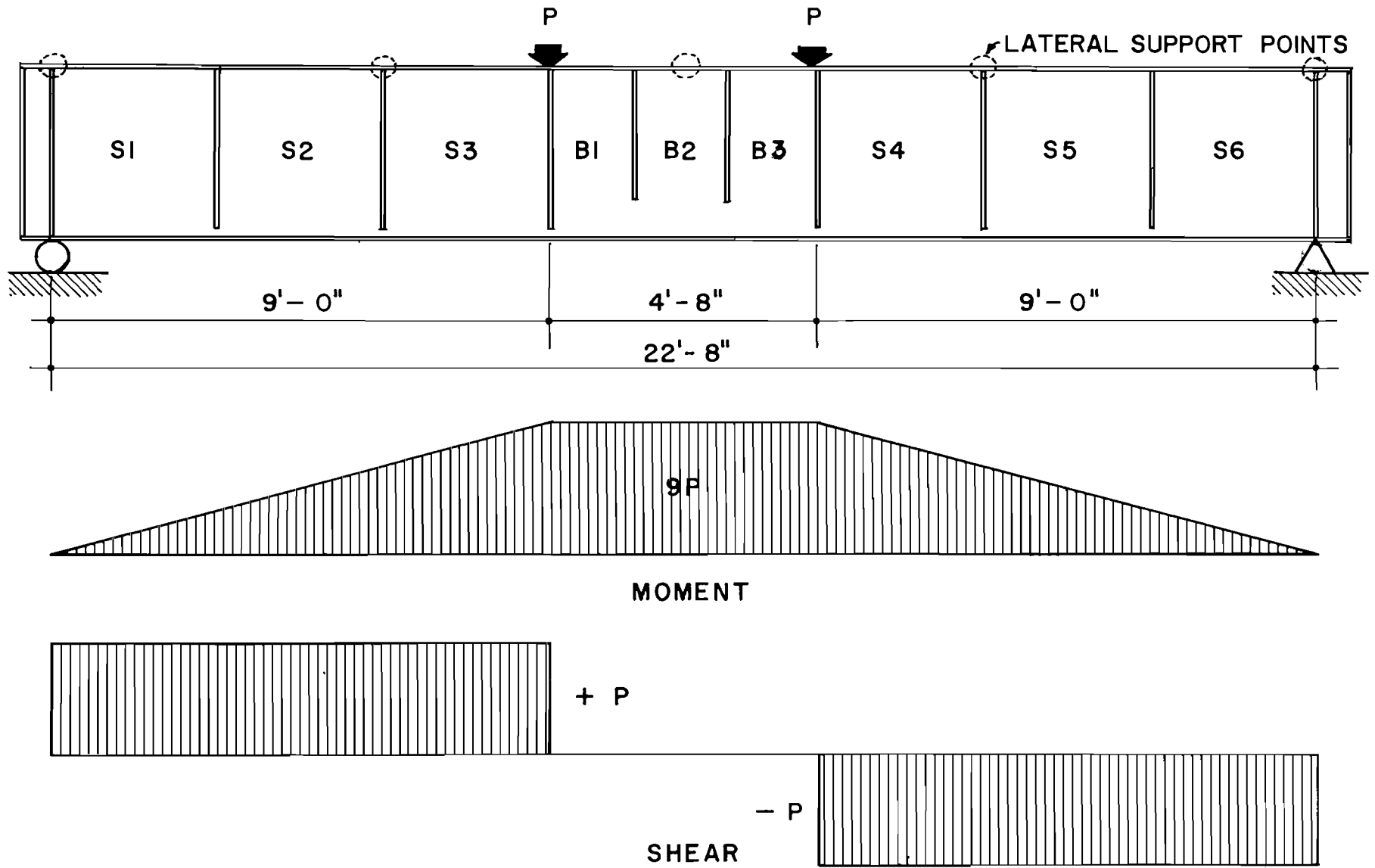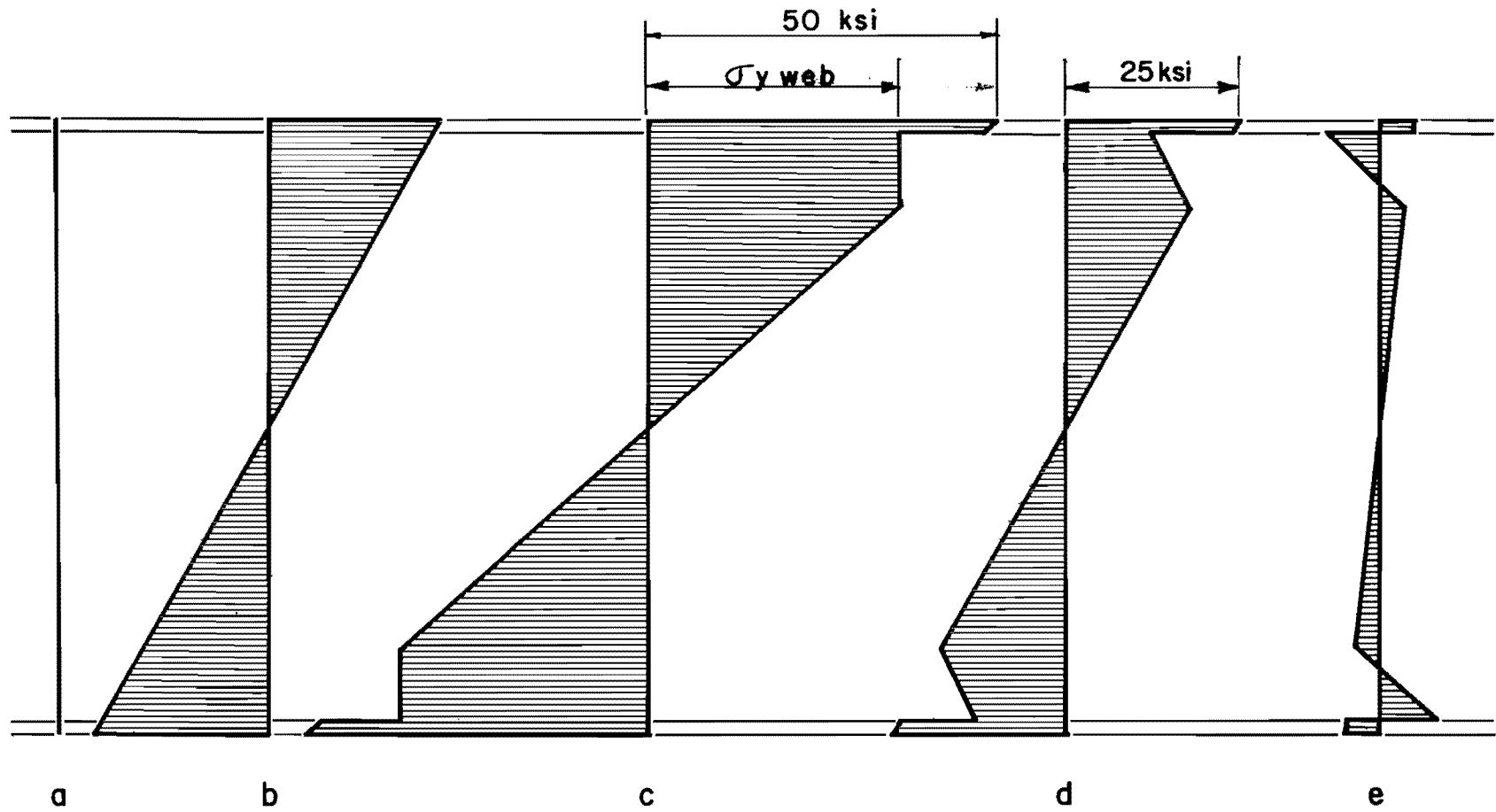
| FIGURE | a | b | c | d | e |
|--------|---|---|---|---|---|
| LOAD NO. | 1 | 4 | 8 | 11 | 14 |
| LOAD | 0 | $P_{min}$ | $P_{max}$ | $P_{min}$ | 0 |

FIG. 4 STRESS DISTRIBUTIONS IN HYBRID PLATE GIRDERS
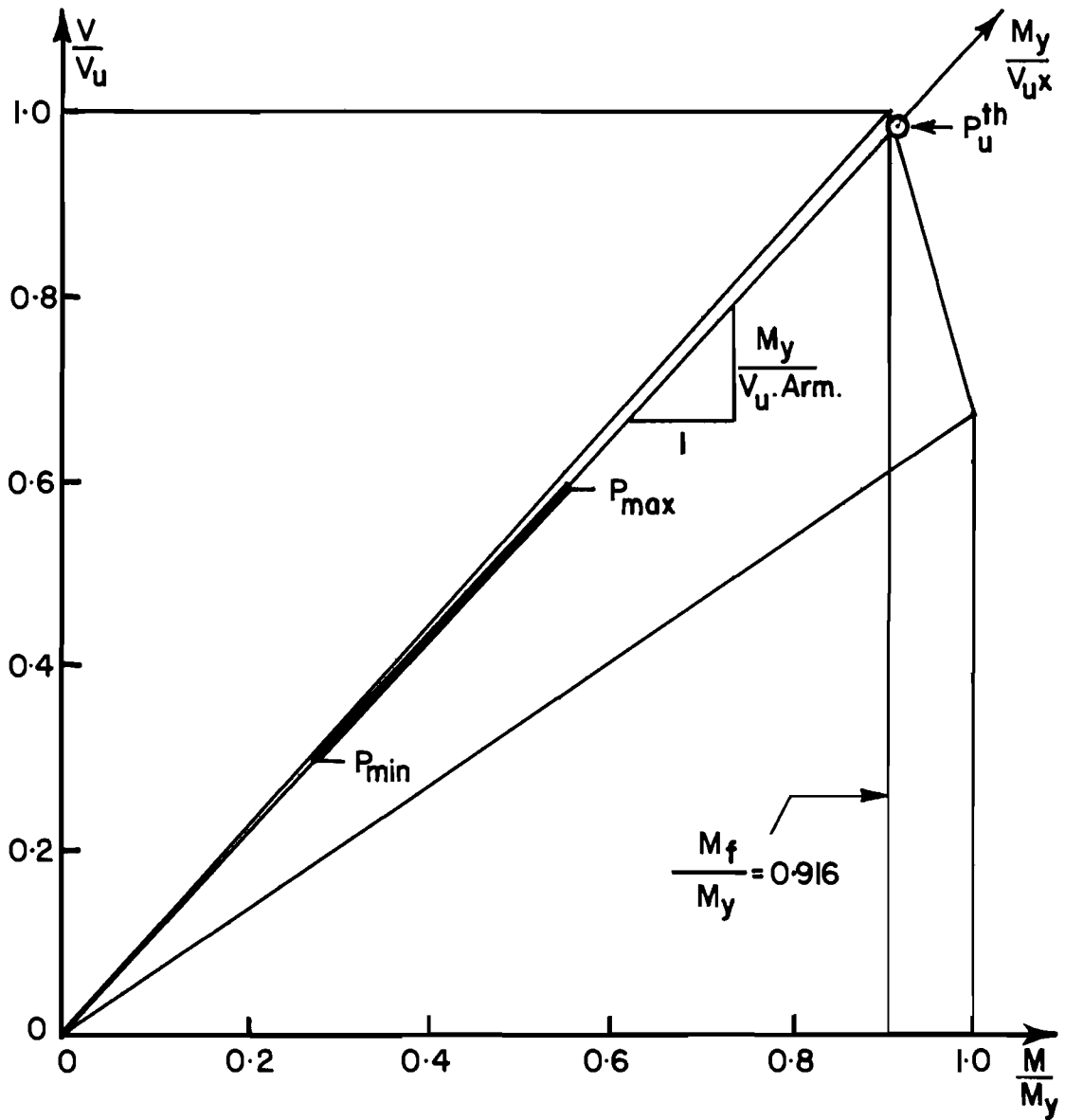
$$\text{SLOPE} = \frac{V/V_u}{M/M_y} = \frac{P/V_u}{P9/M_y} = \frac{M_y\,P}{9\,P V_u} = \frac{M_y}{9\,V_u}$$

M = P(Arm)   (Arm = 9'-0")

$M_y$ = 1498 k.ft.

$V_u$ = 155·8 k.

$$\text{SLOPE} = \frac{1498}{9 \times 155\cdot8} = 1\cdot069$$

FIG. 5    INTERACTION DIAGRAM
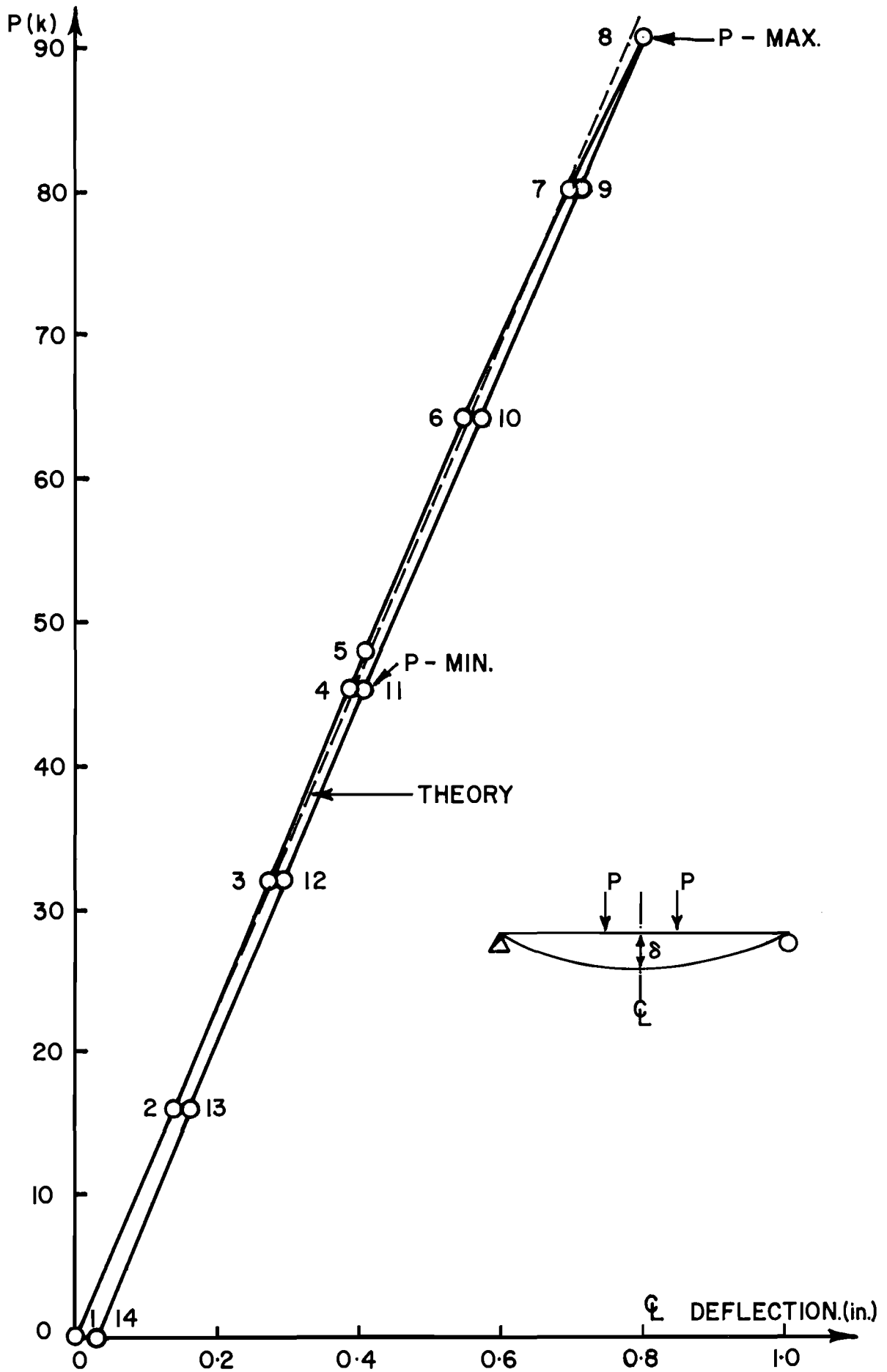
FIG. 6    LOAD  Vs  C̶L DEFLECTION (PRELIMINARY
LOAD  CYCLE  FOR  32550  C2)
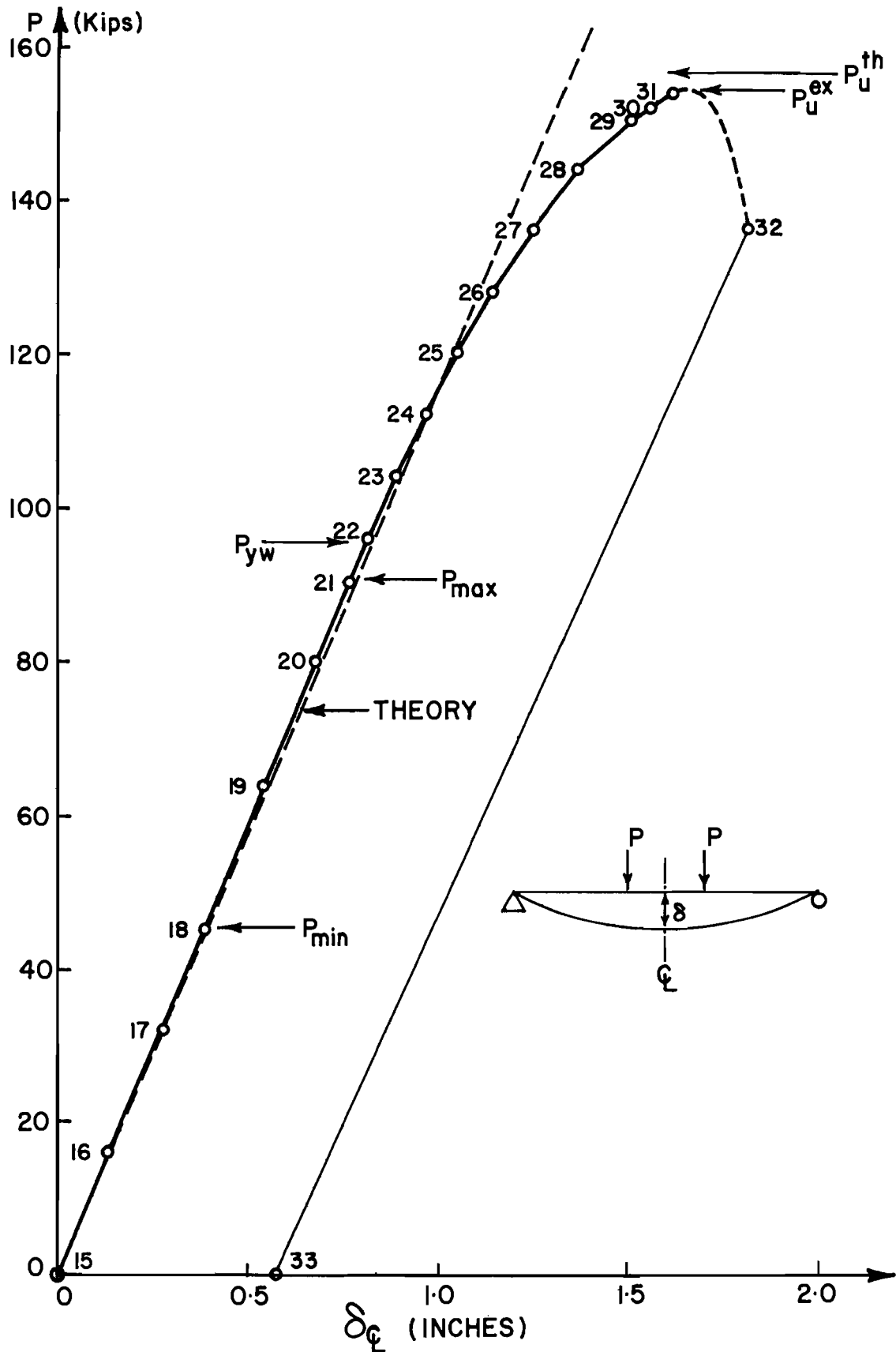
FIG. 7   LOAD-DEFLECTION (32550 C2)
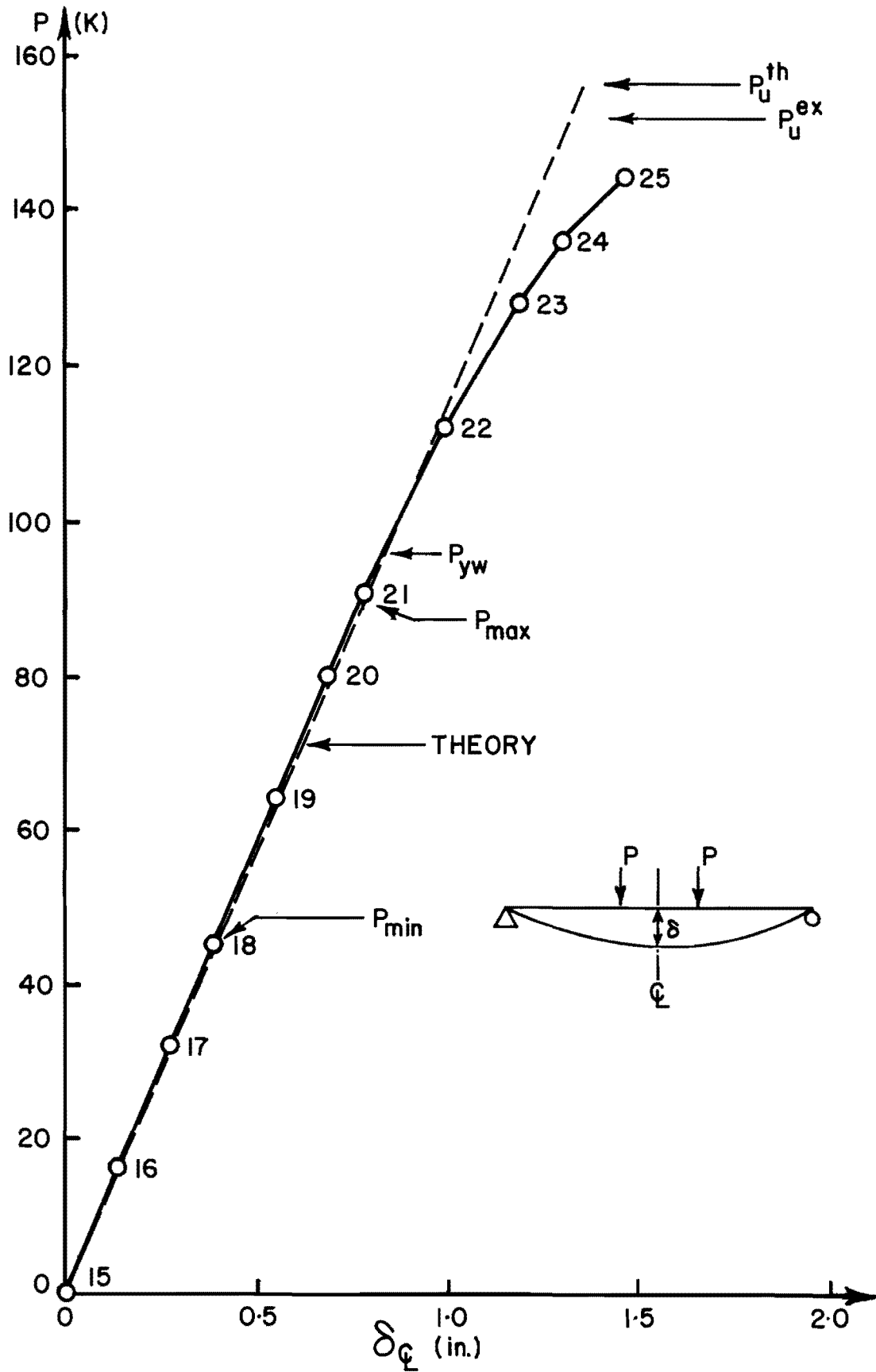
FIG. 8   LOAD Vs ₵ DEFLECTION FOR 32550 C2R
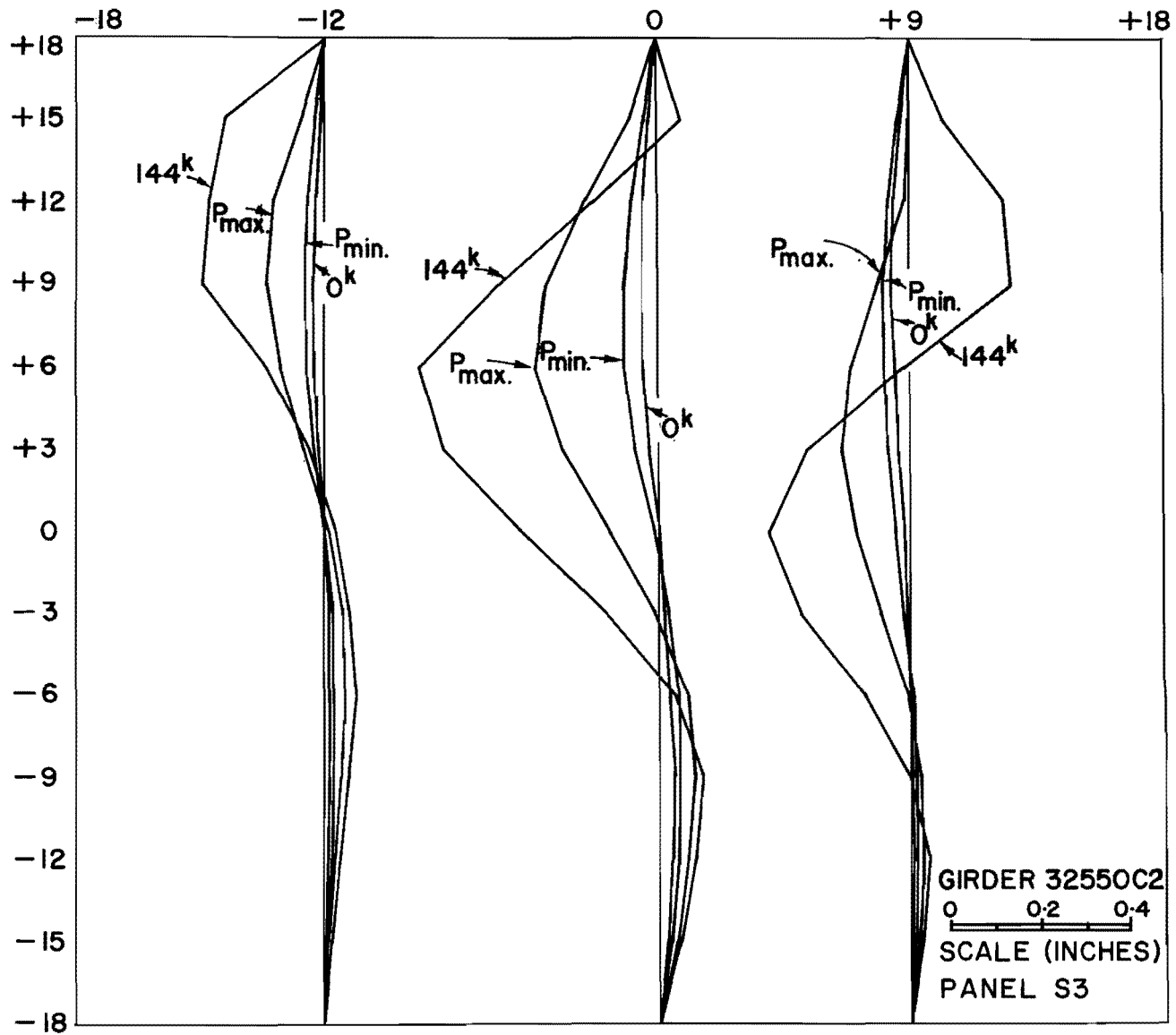
FIG. 9 WEB DEFLECTION

FIG. IO WEB DEFLECTION

FIG. 11  WEB DEFLECTION

34

| S1 | S2 | #3 S3 | | | | S4 #1 | S5 | S6 |

#2
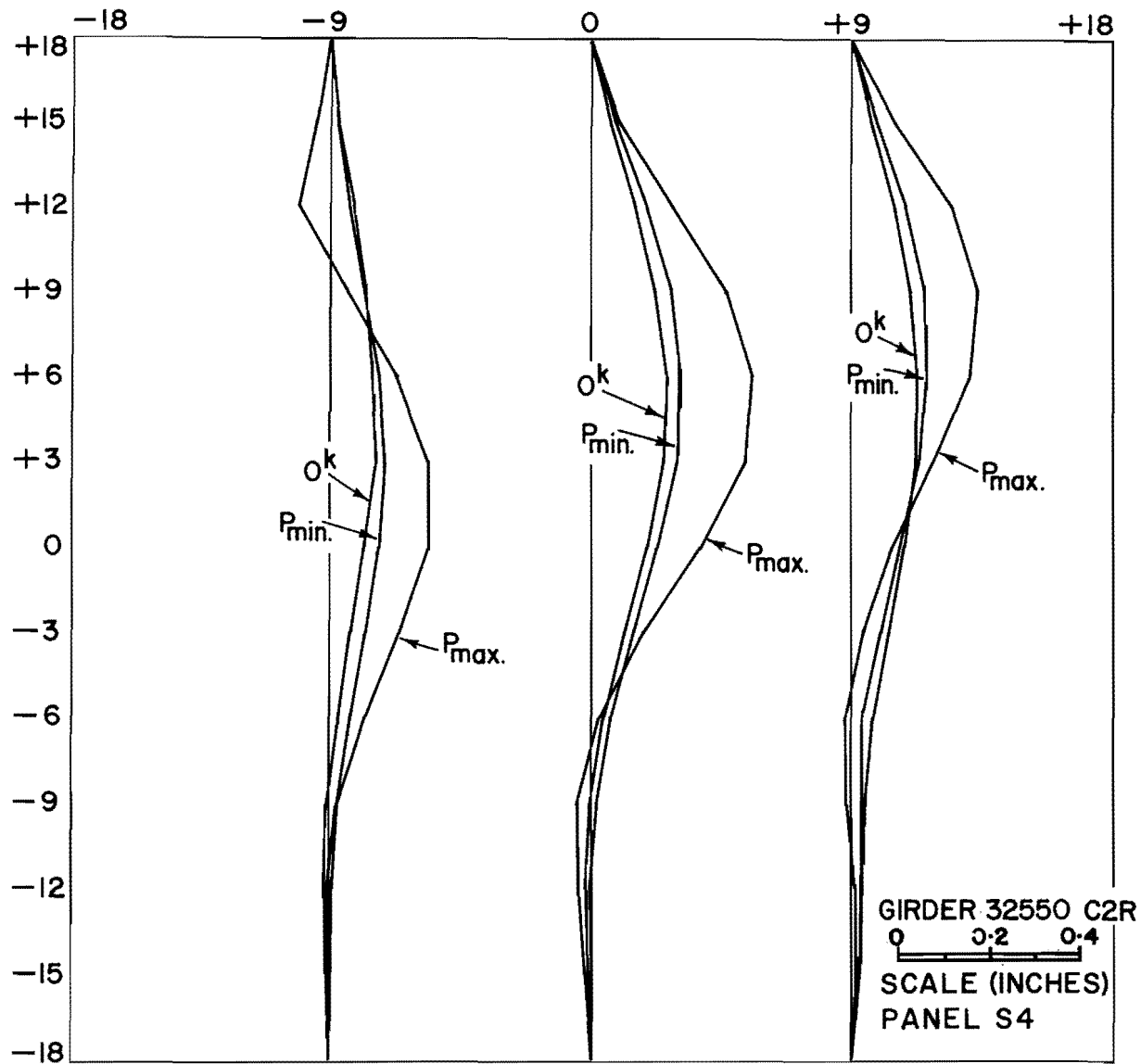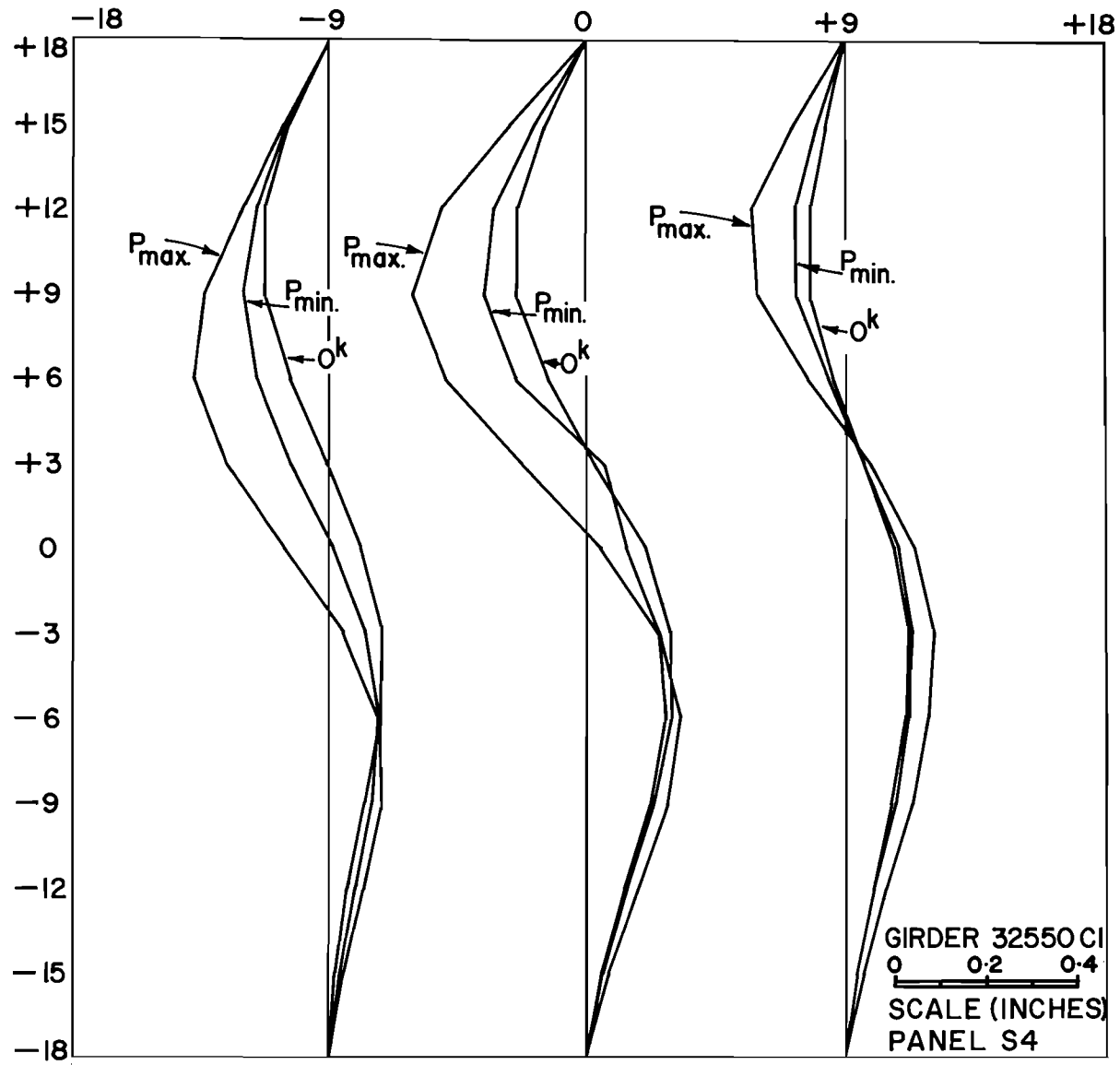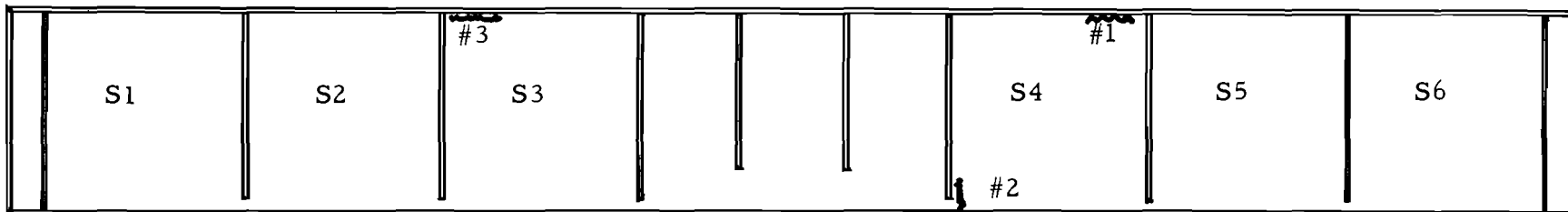
| Crack No. | Began | Both Sides (Cycles) |
|-----------|---------|---------------------|
| 1 | 316,000 | 387,000 |
| 2 | 387,000 | 480,000 |
| Failure | 567,000 | Crack No. 2 penetrates thru to tension flange. |
| Crack #2 Repaired | | |
| 2 | 601,000 | Old Crack #2 reopens |
| 3 | 601,000 | |
| Crack #2 | Repaired again | |
| 2A, 2B | 654,000 | 2A is at same location as Crack #2; 2B near repair. |
| Stopped | 657,000 | |
| Failure due to Crack #2. | | |

Fig. 12 Girder 32550-C2 Crack Locations
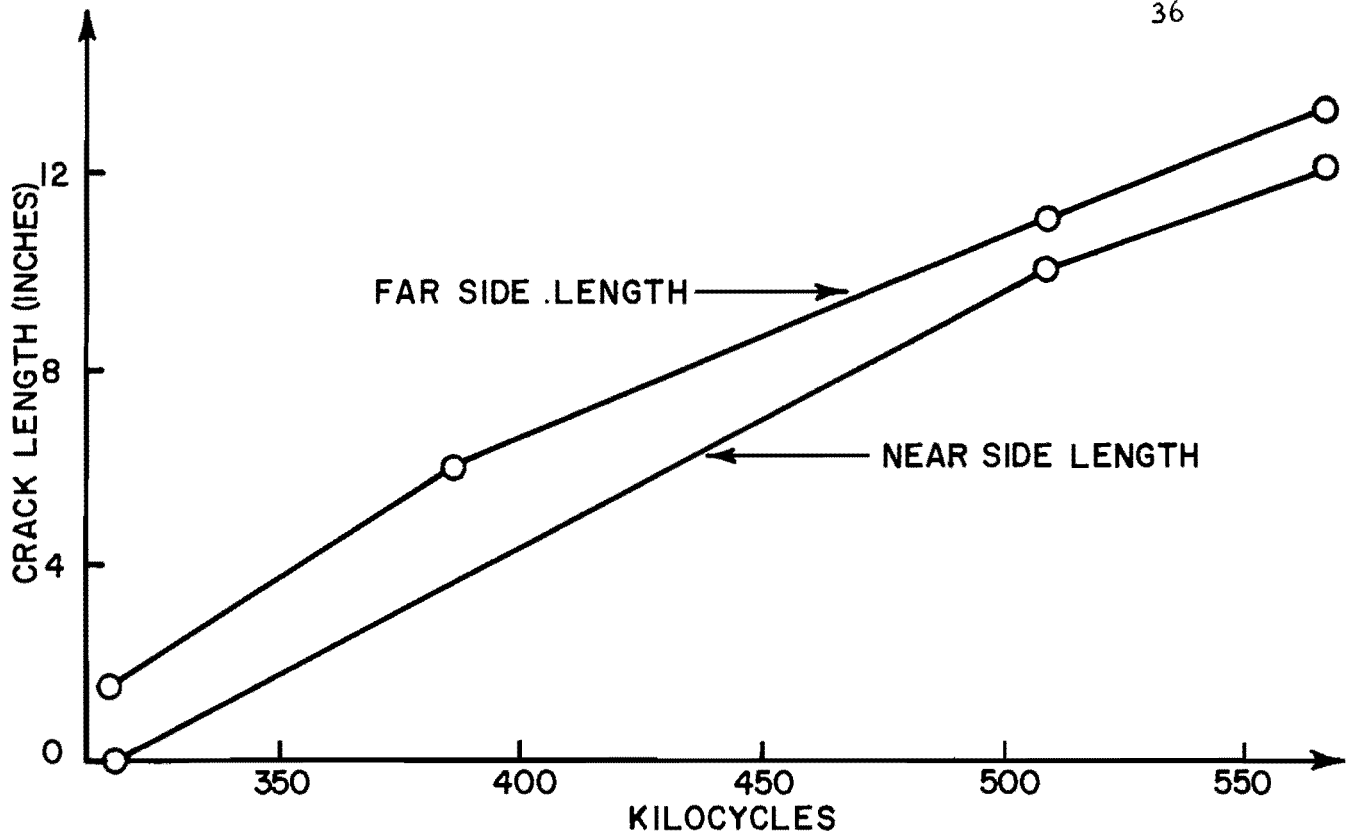
FIG. 13   CRACK PROPAGATION CURVE (CRACK NO.1)32550-C2
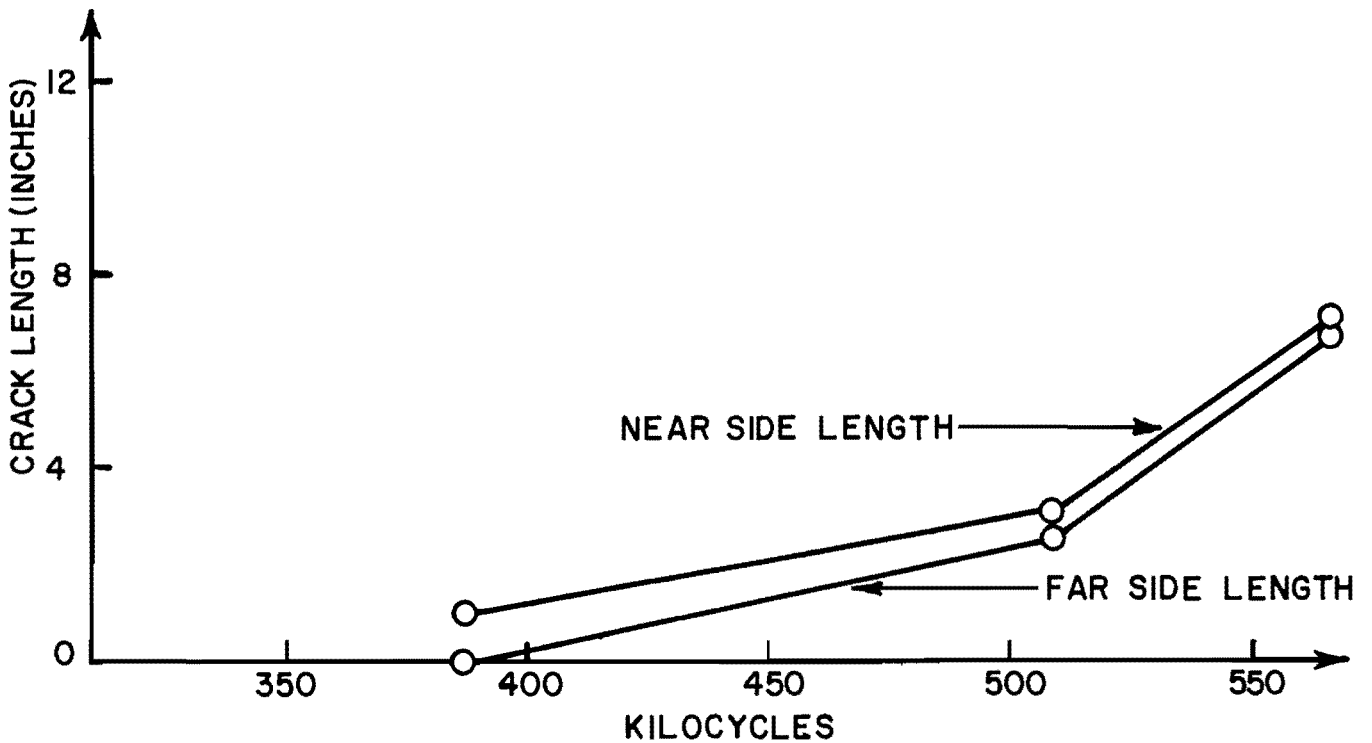


FIG. 14   CRACK PROPAGATION CURVE (CRACK NO.2) 32550-C2
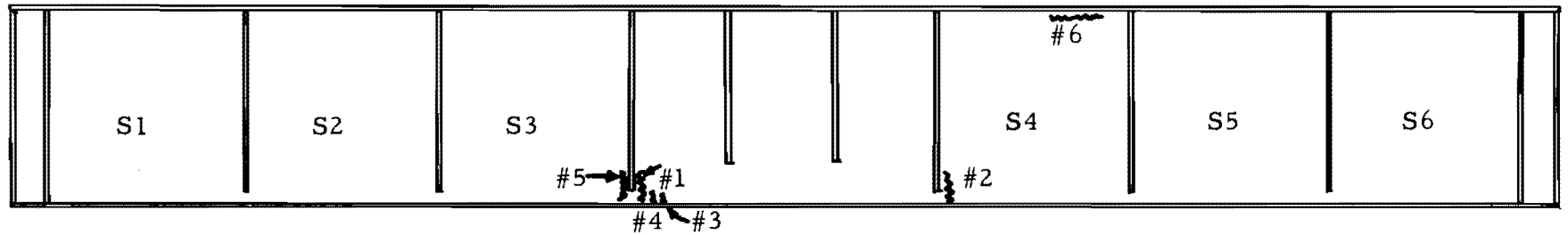
| Crack No. | Began | Both Sides (Cycles) |
|---|---|---|
| 1 | 603,000 | |
| 2 | 656,000 | |
| 3 | 656,000 | |
| Repair of Cracks No. 1, 2, 3 | | |
| 2A | 700,000 | |
| 4 & 5 | 731,000 | 753,000 |
| 1A | 753,000 | |
| Repair of Cracks No. 1A, 2A, 4, 5 | | |
| 4A | 793,000 | |
| 6 | 793,000 | |
| Testing Halted | | |
| Failure due to Crack No. 1 (not in test panel). | | |

Fig. 15

Girder 32550-C2R

Crack Locations
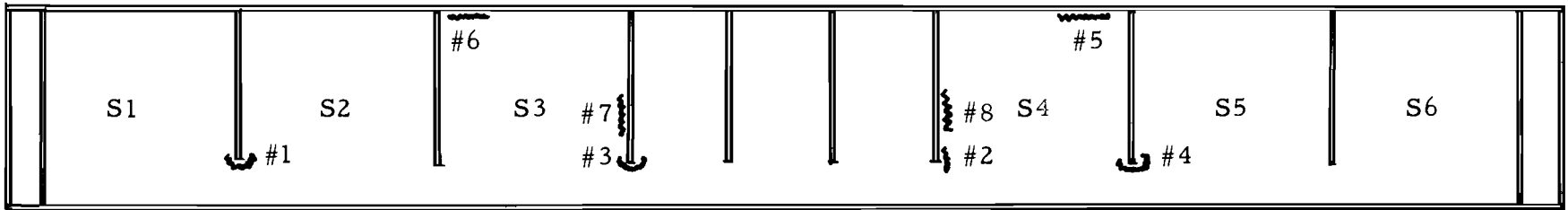
Near Side

| Crack No. | Began | Both Sides |
|-----------|---------|------------|
| 1 | 60,000 | 204,000 |
| 2 | 204,000 | 413,000 |
| 3 | 314,000 | 413,000 |
| 4 | 314,000 | 413,000 |
| 5 | 412,000 | 560,000 |
| 6 | 412,000 | 462,000 |
| 7 | 597,000 | 742,000 |
| 8 | 633,740 | 742,000 |
| Failure | 745,410 | |

Fig. 16 Girder 32550-C 1 Crack Locations

FIGURE 17

U-Shaped Crack under Stiffener (32550-C1)

CRACK NO. 5

412
462
634
671
715
742

CRACK NO. 8

745
634

NO. 2 MEETS NO. 8 AT 745,000 CYCLES
AND PANEL BUCKLES

CRACK NO. 2

426 634 671 715 742 745

NUMBERS INDICATE KILOCYCLES

SPECIMEN 32550 CI
NEAR SIDE
CRACKS 2,5,8
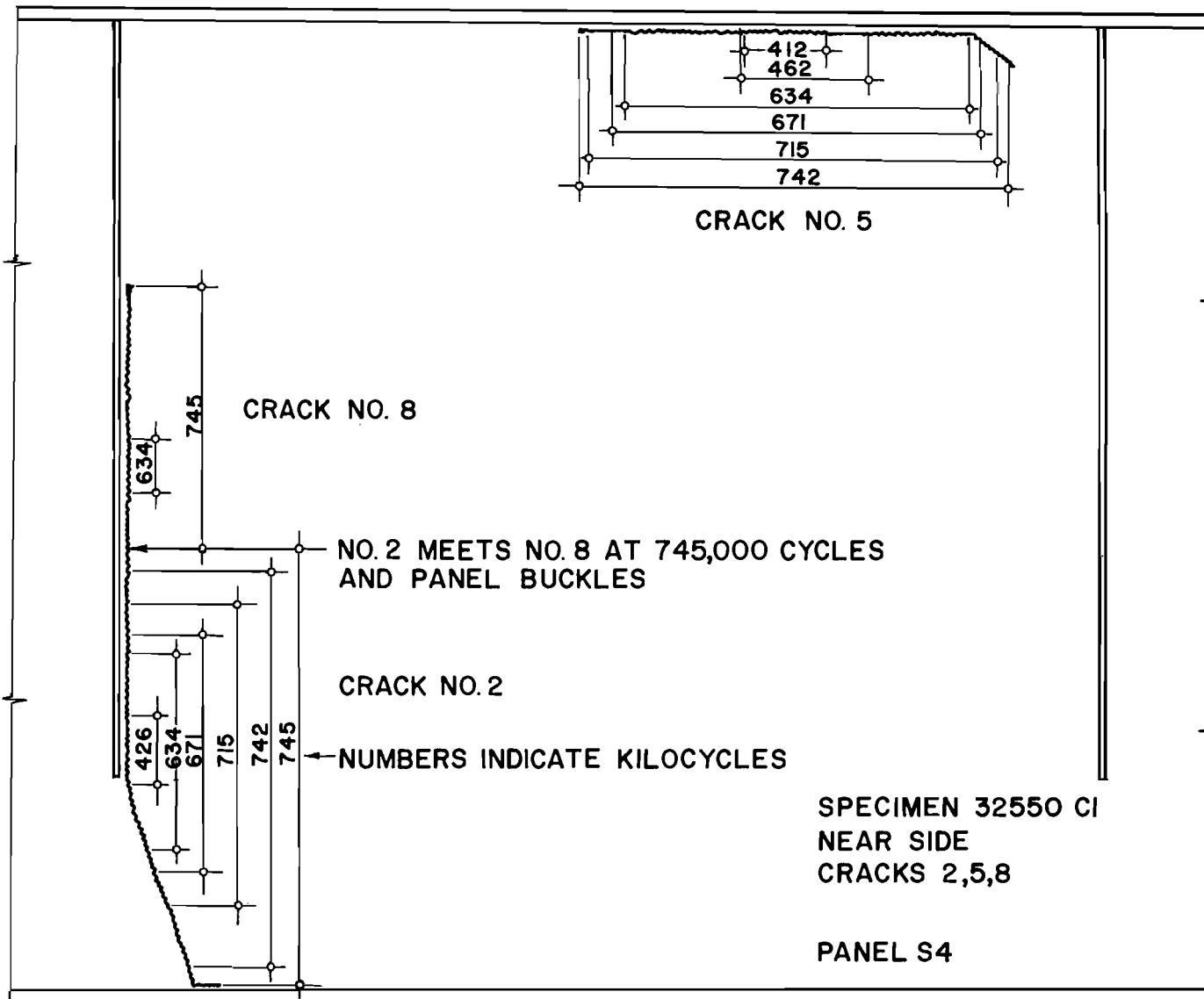
PANEL S4

FIG. 18  CRACK GROWTH
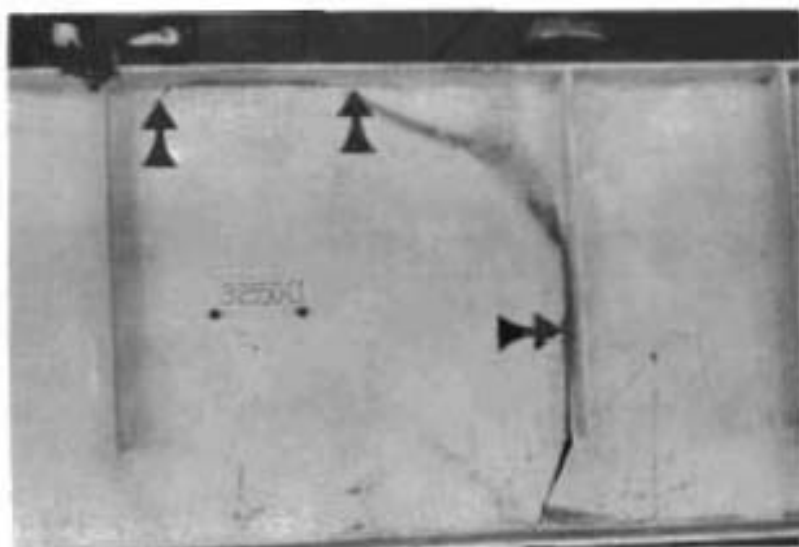
FIGURE 19

Panel S4 after Fatigue Test (32550-C1)
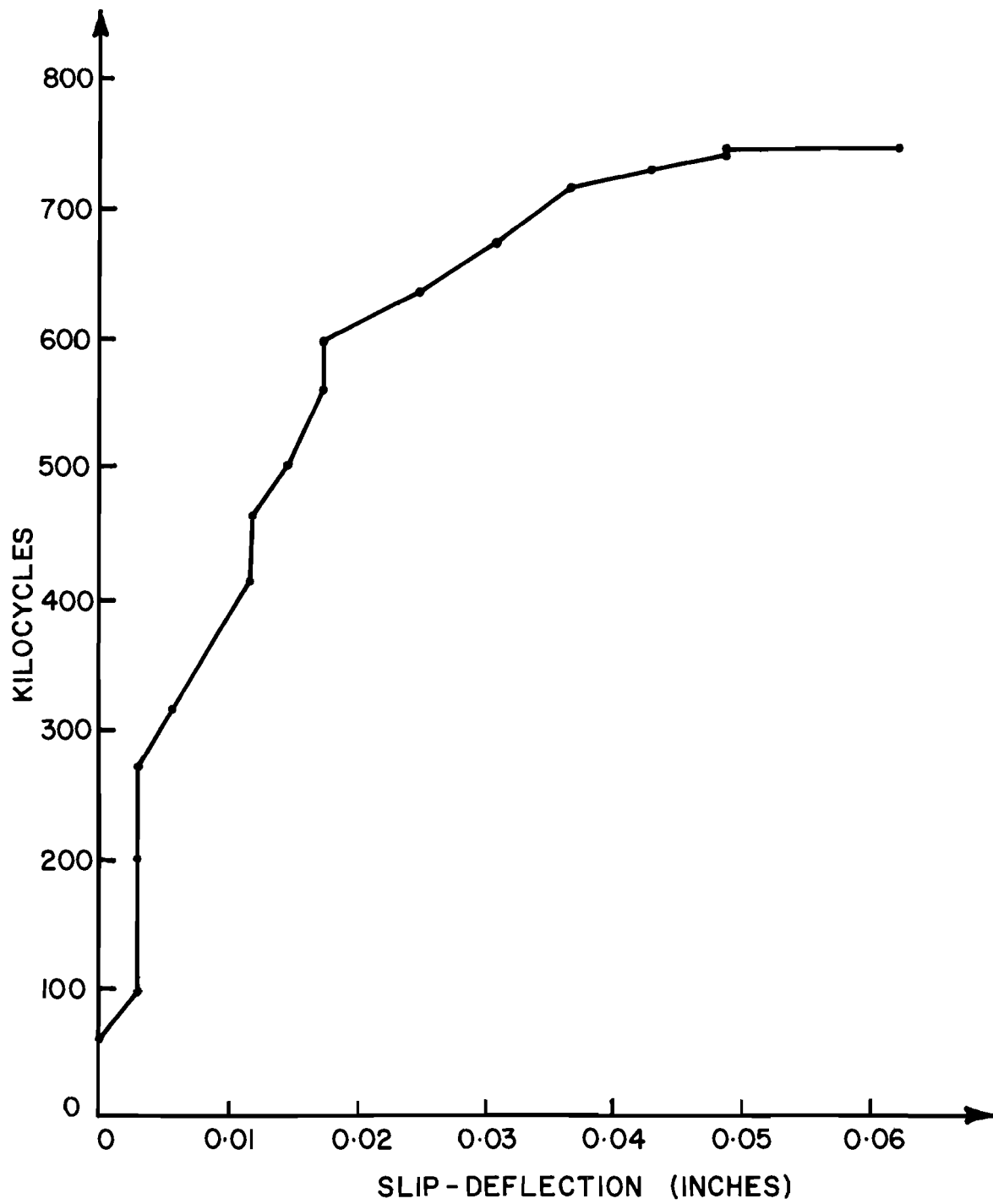
FIG. 20 SLIP - DEFLECTION CURVE FOR 32550 - CI
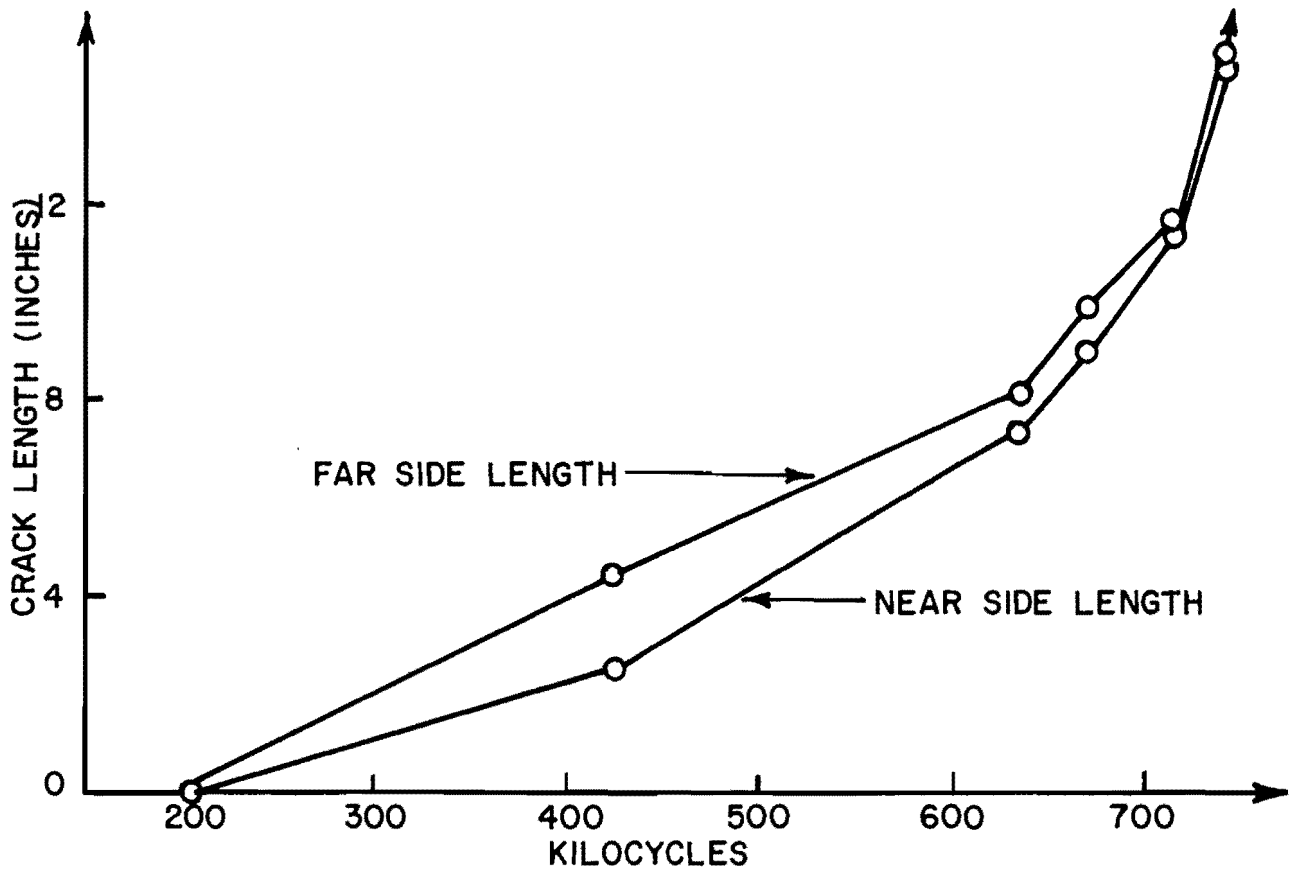
FIG. 21    CRACK PROPAGATION CURVE (CRACK NO.2) 32550·CI
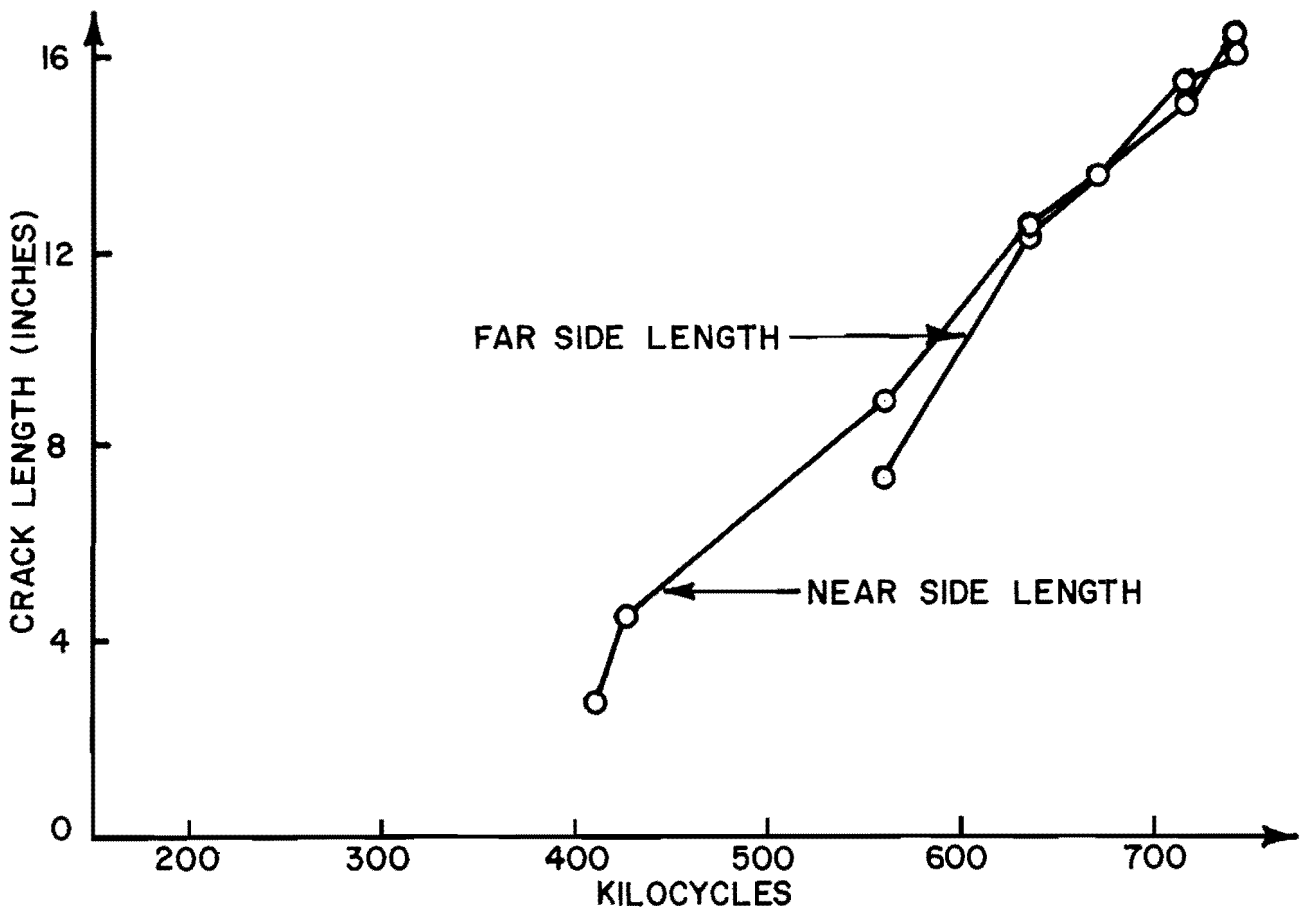


FIG. 22 CRACK PROPAGATION CURVE (CRACK NO.5) 32550-CI
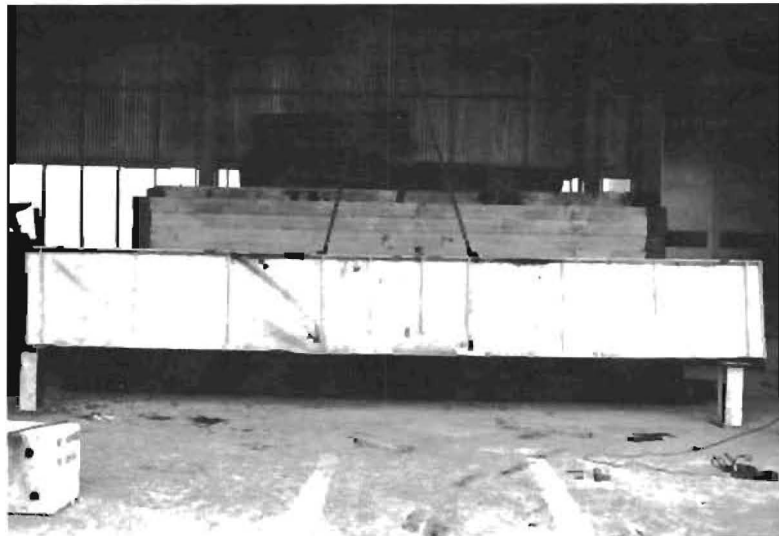
FIGURE 23

Girder 32550-C2 after Failure
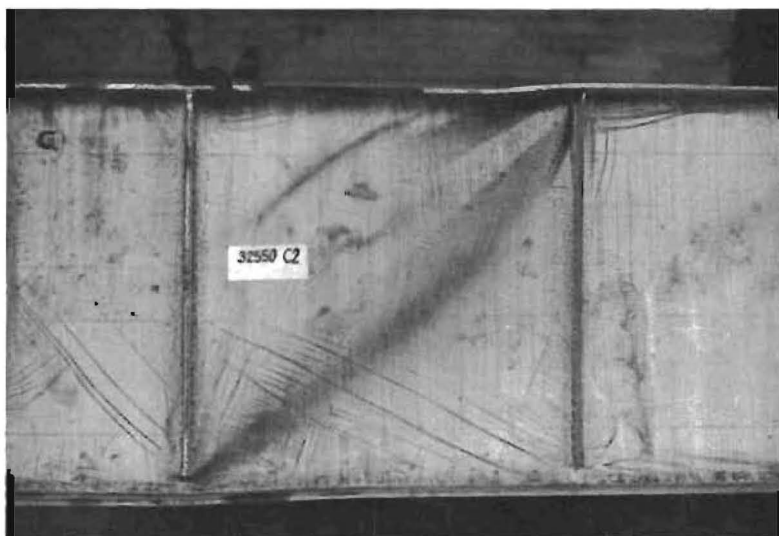
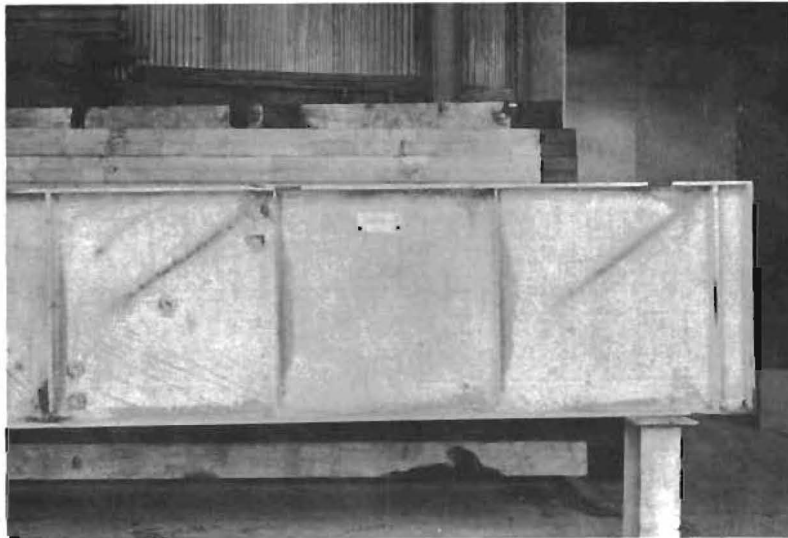

FIGURE 24

Shear Failure in Panel S3 (32550-C2)
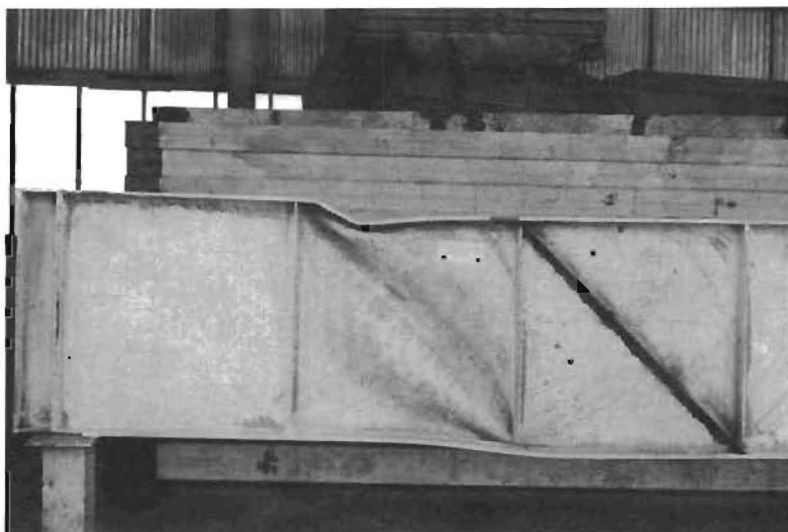
FIGURE 25

"Diagonal" Yielding in 32550-C2R
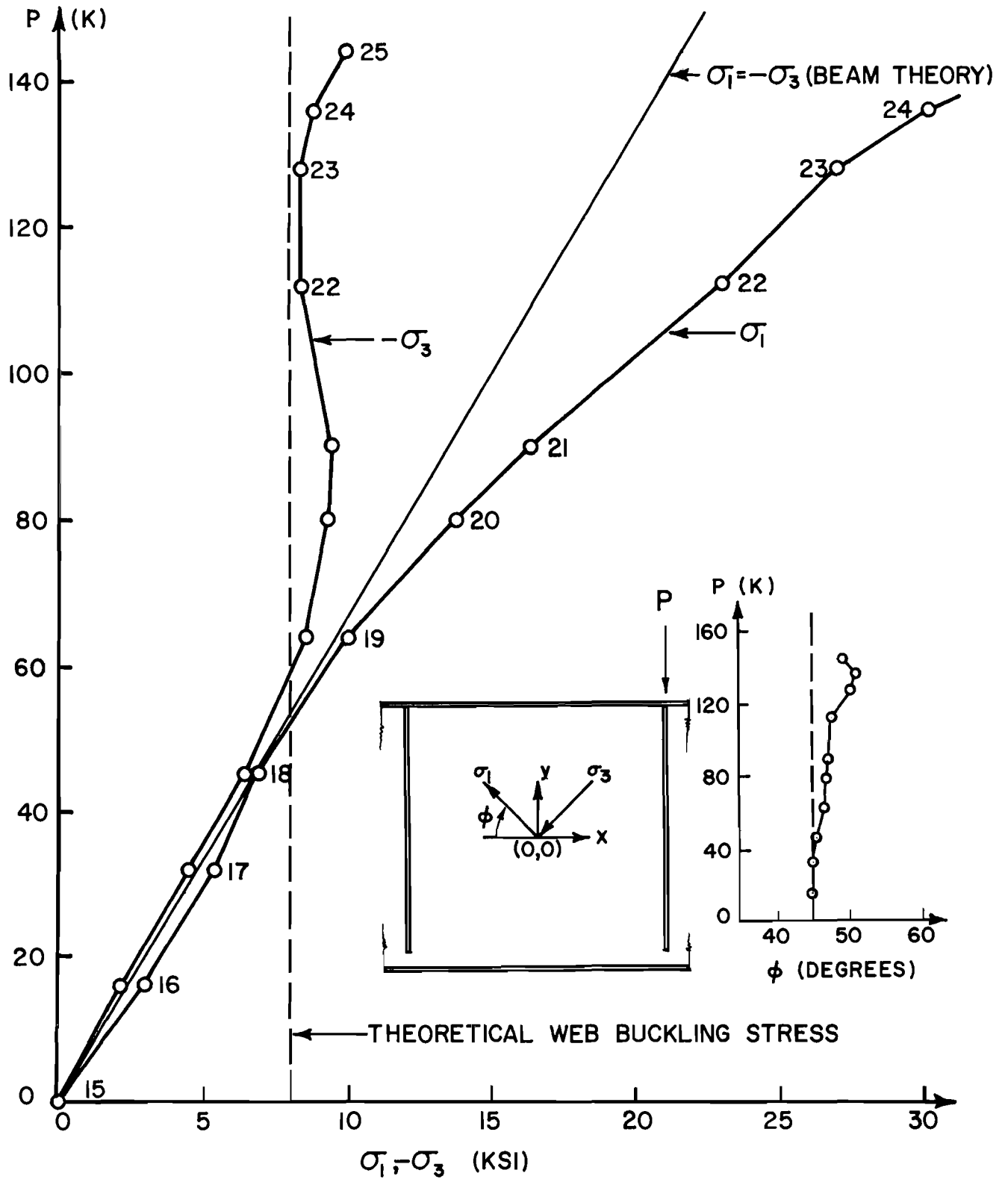


FIGURE 26

Panels S6, S5, S4 (l. tor.) in 32550-C2R
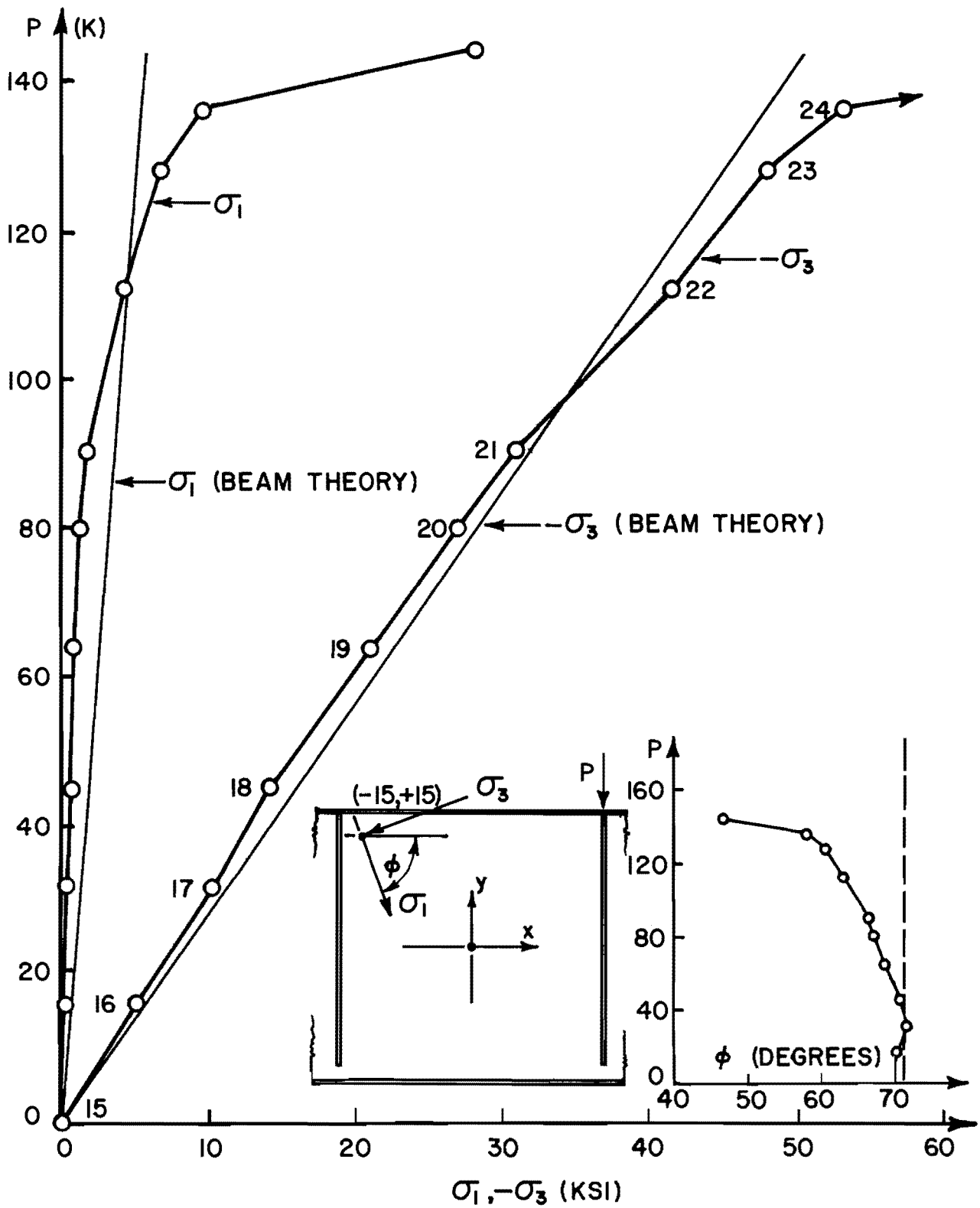
FIG. 27   PRINCIPAL STRESSES IN PANEL S3
( 32550 - C2R )

FIG. 28 PRINCIPAL STRESSES IN PANEL S3
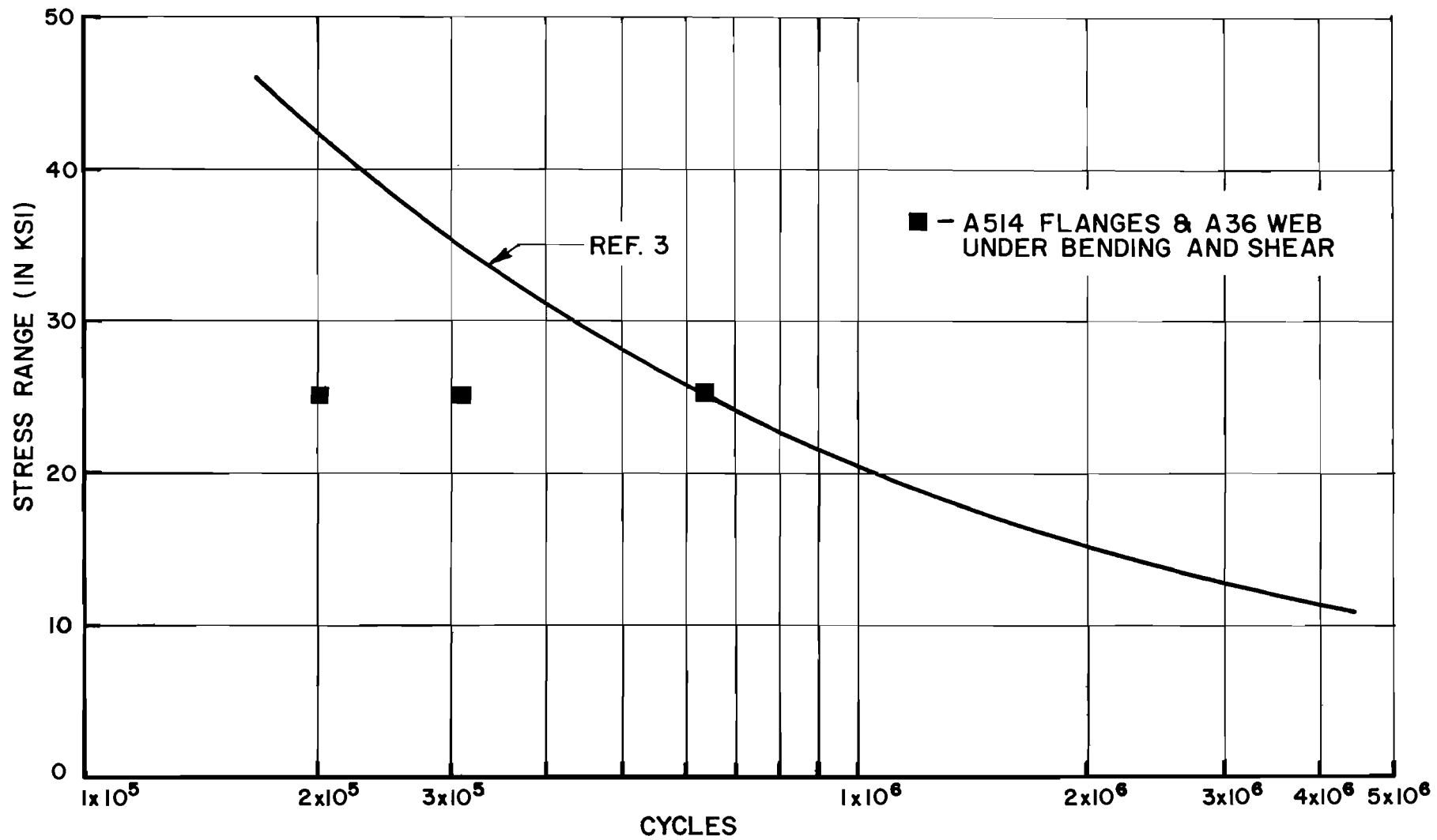( 32550 – C2R )

FIG. 29    S-N   CURVE   FOR   BENDING   TESTS

48

# 8. REFERENCES

1. A. A. Toprac
   "Plate Girders with High Strength Steel Flanges,"
   Proceedings, 1961 National Engineering Conference,
   American Institute of Steel Construction.

2. A. A. Toprac
   "Fatigue Strength of Full Size Hybrid Girders -
   A Progress Report," Proceedings, 1963 National
   Engineering Conference, American Institute of
   Steel Construction.

3. H. S. Lew and A. A. Toprac
   "Fatigue Tests of Welded Hybrid Plate Girders
   Under Constant Moment," Research Report 77-2F,
   Center for Highway Research, The University of
   Texas, Austin, January 1967.

4. Y. Kurobane, D. J. Fielding, and A. A. Toprac
   "Additional Fatigue Tests of Hybrid Plate Girders
   Under Pure Bending Moment," Research Report
   96-1, Center for Highway Research, The Univer-
   sity of Texas, Austin, May, 1967.

5. K. Basler and B. Thurlimann
   "Strength of Plate Girders in Bending," Proc.
   ASCE, 87, ST 6, August, 1961.

6. K. Basler
   "Strength of Plate Girders in Shear," Proc. ASCE,
   87, ST 7, October, 1961.

7. K. Basler
   "Strength of Plate Girders Under Combined Bend-
   ing and Shear," Proc. ASCE, 87, ST 7, October
   1961.

8. B. T. Yen and J. A. Mueller
   "Fatigue Tests of Large-Size Welded Plate Girders,"
   Welding Research Council Bulletin No. 118, Novem-
   ber, 1966.